Expanding the diversity of bacterioplankton isolates and modeling isolation efficacy with large scale dilution-to-extinction cultivation

Michael W. Henson[1,#], V. Celeste Lanclos[1], David M. Pitre[2], Jessica Lee Weckhorst[2,†], Anna M. Lucchesi[2], Chuankai Cheng[1], Ben Temperton[3*], and J. Cameron Thrash[1*]

[1]Department of Biological Sciences, University of Southern California, Los Angeles, CA 90089, U.S.A.
[2]Department of Biological Sciences, Louisiana State University, Baton Rouge, LA 70803, U.S.A.
[3]School of Biosciences, University of Exeter, Stocker Road, Exeter, EX4 4QD, U.K.
[#]Current affiliation: Department of Geophysical Sciences, University of Chicago, Chicago, IL 60637, U.S.A.
[†]Current affiliation: Quantitative and Computational Biosciences Program, Baylor College of Medicine, Houston, TX 77030, U.S.A.

*Correspondence:

J. Cameron Thrash
thrash@usc.edu

Ben Temperton
b.temperton@exeter.ac.uk

Running title: Evaluation of large-scale DTE cultivation

Keywords: dilution-to-extinction, cultivation, bacterioplankton, LSUCC, microbial ecology, coastal microbiology

Abstract

Cultivated bacterioplankton representatives from diverse lineages and locations are essential for microbiology, but the large majority of taxa either remain uncultivated or lack isolates from diverse geographic locales. We paired large scale dilution-to-extinction (DTE) cultivation with microbial community analysis and modeling to expand the phylogenetic and geographic diversity of cultivated bacterioplankton and to evaluate DTE cultivation success. Here, we report results from 17 DTE experiments totaling 7,820 individual incubations over three years, yielding 328 repeatably transferable isolates. Comparison of isolates to microbial community data of source waters indicated that we successfully isolated 5% of the observed bacterioplankton community throughout the study. 43% and 26% of our isolates matched operational taxonomic units and amplicon single nucleotide variants, respectively, within the top 50 most abundant taxa. Isolates included those from previously uncultivated clades such as SAR11 LD12 and *Actinobacteria* acIV, as well as geographically novel members from other ecologically important groups like SAR11 subclade IIIa, SAR116, and others; providing the first isolates in eight putatively new genera and seven putatively new species. Using a newly developed DTE cultivation model, we evaluated taxon viability by comparing relative abundance with cultivation success. The model i) revealed the minimum attempts required for successful isolation of taxa amenable to growth on our media, and ii) identified possible subpopulation viability variation in abundant taxa such as SAR11 that likely impacts cultivation success. By incorporating viability in experimental design, we can now statistically constrain the effort necessary for successful cultivation of specific taxa on a defined medium.

Importance

Even before the coining of the term “great plate count anomaly” in the 1980s, scientists had noted the discrepancy between the number of microorganisms observed under the microscope and the number of colonies that grew on traditional agar media. New cultivation approaches have reduced this disparity, resulting in the isolation of some of the “most wanted” bacterial lineages. Nevertheless, the vast majority of microorganisms remain uncultured, hampering progress towards answering fundamental biological questions about many important microorganisms. Furthermore, few studies have evaluated the underlying factors influencing cultivation success, limiting our ability to improve cultivation efficacy. Our work details the use of dilution-to-extinction (DTE) cultivation to expand the phylogenetic and geographic diversity of available axenic cultures. We also provide a new model of the DTE approach that uses cultivation results and natural abundance information to predict taxon-specific viability and iteratively constrain DTE experimental design to improve cultivation success.

Introduction

Axenic cultures of environmentally important microorganisms are critical for fundamental microbiological investigation, including generating physiological information about environmental tolerances, determining organismal-specific metabolic and growth rates, testing hypotheses generated from *in situ* 'omics observations, and experimentally examining microbial interactions. Research using important microbial isolates has been critical to a number of discoveries such as defining microorganisms involved in surface ocean methane saturation (1–3), the role of proteorhodopsin in maintaining cellular functions during states of carbon starvation (4, 5), the complete nitrification of ammonia within a single organism (6), and identifying novel metabolites and antibiotics (7–10). However, the vast majority of taxa remain uncultivated (11–13), restricting valuable experimentation on such topics as genes of unknown function, the role of analogous gene substitutions in overcoming auxotrophy, and the multifaceted interactions occurring in the environment inferred from sequence data (11, 14–16).

The quest to bring new microorganisms into culture, and the recognition that traditional agar-plate based approaches have limited success (17–19), have compelled numerous methodological advances spanning a wide variety of techniques like diffusion chambers, microdroplet encapsulation, and slow acclimatization of cells to artificial media (20–25). Dilution-to-extinction (DTE) cultivation using sterile seawater as the medium has also proven highly successful for isolating bacterioplankton (26–32). Pioneered by Don Button and colleagues for the cultivation of oligotrophic bacteria, this method essentially pre-isolates organisms after serial dilution by separating individual or small groups of cells into their own incubation vessel (32, 33). This prevents slow-growing, obligately oligotrophic bacterioplankton from being outcompeted by faster-growing organisms, as would occur in enrichment-based isolation methods like those that would target aerobic heterotrophs. It is also a practical method for taxa that cannot grow on solid media. Natural seawater media provide these taxa with the same chemical surroundings from which they are collected, reducing the burden of anticipating all the relevant compounds required for growth (33).

Improvements to DTE cultivation in multiple labs have increased the number of inoculated wells and decreased the time needed to detect growth (26, 28, 34), thereby earning the moniker "high-throughput culturing" (26, 28). We (35) and others (30) have also adapted DTE culturing by incorporating artificial media in place of natural seawater media to successfully isolate abundant bacterioplankton. Thus far, DTE culturing has led to isolation of many numerically abundant marine and freshwater groups such as marine SAR11 *Alphaproteobacteria* (28, 29, 34–36), the freshwater SAR11 LD12 clade (29), SUP05/Arctic96BD-19 *Gammaproteobacteria* (37–39), OM43 *Betaproteobacteria* (26, 27, 31, 40, 41), HIMB11-Type Roseobacter spp. (35, 42), numerous so-called Oligotrophic Marine *Gammaproteobacteria* (43), and acI *Actinobacteria* (44).

Despite the success of DTE cultivation, many taxa continue to elude domestication (11–13, 16). Explanations include a lack of required nutrients or growth factors in media (20, 45–49) and biological phenomena such as dormancy and/or phenotypic heterogeneity within populations (47, 48, 50–56). However, there have been few studies empirically examining the factors underlying isolation success in DTE cultivation experiments (34, 57, 58), restricting our ability to determine the relative importance of methodological vs. biological influences on cultivation reliability for any given organism. Moreover, even for those taxa that we have successfully cultivated, in many cases we lack geographically diverse strains, restricting comparisons of the phenotypic and genomic diversity that may influence taxon-specific cultivability.

We undertook a three-year cultivation effort in the coastal northern Gulf of Mexico (nGOM), from which we lack representatives of many common bacterioplankton groups, to provide new model organisms for investigating microbial function, ecology, biogeography, and evolution. Simultaneously, we paired our cultivation efforts with 16S rRNA gene amplicon analyses to compare cultivation results with the microbial communities in the source waters. We have previously reported on the success of our artificial media in obtaining abundant taxa over the course of the first seven experiments from this campaign (35). Here, we expand our report to include cultivation results from a total of seventeen experiments, and update the classic viability calculations of Button *et al.* (33) with a new model to estimate the viability of individual taxa using relative abundance information. New isolates belonged to cultivated groups in eight putatively novel genera and seven putatively novel species in previously cultivated genera and expanded cultured geographic representation for many important clades like SAR11. Additionally, using model-based predictions, we identified possible taxon-specific viability variation that can influence cultivation success. By incorporating these new viability estimates into the model, our method facilitates statistically-informed experimental design for targeting individual taxa, thereby reducing uncertainty for future culturing work (59).

Material and Methods

Sampling

Surface water samples were collected at six different sites once a year for three years, except for Terrebonne Bay, which was collected twice. The sites sampled were Lake Borgne (LKB; Shell Beach, LA), Bay Pomme d'Or (JLB; Buras, LA), Terrebonne Bay (TBON; Cocodrie, LA), Atchafalaya River Delta (ARD; Franklin, LA), Freshwater City (FWC; Kaplan, LA), and Calcasieu Jetties (CJ; Cameron, LA) (lat/long coordinates provided in Table S1). Water collection for biogeochemical and biological analysis followed the protocol in (35). Briefly, we collected surface water in a sterile, acid-washed polycarbonate bottle. Duplicate 120 ml water samples were filtered serially through 2.7 µm Whatman GF/D (GE Healthcare, Little Chalfort, UK) and 0.22 µm Sterivex (Millipore, Massachusetts, USA) filters and placed on ice until transferred to -20˚C in the laboratory (maximum 3 hours on ice). The University of Washington Marine Chemistry Laboratory analyzed duplicate subsamples of 50 ml 0.22 µm-filtered water collected in sterile 50 ml falcon tubes (VWR, Pennsylvania, USA) for concentrations of SiO_4, PO_4^{3-}, NH_4^+, NO_3^-, and NO_2^-. Samples for cell counts were filtered through a 2.7 µm GF/D filter, fixed with 10% formaldehyde, and stored on ice until enumeration (maximum 3 hours). Temperature, salinity, pH, and dissolved oxygen were measured using a handheld YSI 556 multiprobe system (YSI Inc., Ohio, USA). All metadata is available in Table S1.

Dilution-to-extinction culturing and propagation

Isolation, propagation, and identification of isolates were completed as previously reported (29, 35, 60). A subsample of 2.7 µm filtered surface water was stained with 1X SYBR Green (Lonza, Basal, Switzerland) using a repeat pipettor and disposal tip (Gilson, Wisconsin, USA), and enumerated using a Guava Easycyte 5HT HPL flow cytometer (Millipore, Massachusetts, USA) as described (60). After serial dilution to a predicted 1-3 cells·µl^{-1}, 2 µl water was inoculated into five, 2 mL 96-well PTFE plates (Radleys, Essex, UK) containing 1.7 ml artificial seawater medium (Table S1) using a 20 uL multichannel pipet (Gilson, Wisconsin, USA) to achieve an estimated 1-3 cells·well^{-1} (Table 1). The salinity of the medium was chosen to match *in situ*

salinity after experiment JLB (January 2015) (Tables 1, S1). After year two, a second generation of media, designated MWH, was designed to incorporate additional important osmolytes, reduced sulfur compounds, and other constituents (Tables 1, S1) potentially necessary for *in vitro* growth of uncultivated clades (49, 61–67). The four corner wells of each plate were left uninoculated as negative controls for every experiment. Plates were covered using sterile, PTFE-coated silicon 96-well plate mats (Thermo Scientific, Massachusetts, USA). Cultures were incubated at *in situ* temperatures (Table S1) in the dark for three to six weeks and evaluated for positive growth ($> 10^4$ cells·ml^{-1}) by flow cytometry. 200 µl from positive wells was transferred using a 200 µL single channel pipet (Gilson, Wisconsin, USA) to duplicate 125 ml polycarbonate flasks (Corning, New York, USA) containing 50 ml of medium (29, 35, 60). At FWC, FWC2, JLB2c, and JLB3, not all positive wells were transferred because of the large number of positive wells. At each site, 48/301, 60/403, 60/103, and 60/146 of the positive wells were transferred, respectively, selected using flow cytometry signatures with $< 10^2$ green fluorescence and $< 10^2$ side scatter that maximized our chances of isolating small microorganisms that encompass many of the most abundant and most wanted taxa, like SAR11, using our settings (60).

Culture identification

Cultures reaching $\geq 1 \times 10^5$ cells·ml^{-1} had 35 ml of the 50 ml volume filtered for identification via 16S rRNA gene PCR onto 25 mm 0.22-µm polycarbonate filters (Millipore, Massachusetts, USA). DNA extractions were performed using the MoBio PowerWater DNA kit (QIAGEN, Massachusetts, USA) following the manufacturer's instructions and eluted in sterile water. The 16S rRNA gene was amplified as previously reported in Henson et al. 2016 (35) and sequenced at Michigan State University Research Technology Support Facility Genomics Core. Evaluation of Sanger sequence quality was performed with 4Peaks (v. 1.7.1) (http://nucleobytes.com/4peaks/) and forward and reverse complement sequences (converted via http://www.bioinformatics.org/sms/rev_comp.html) were assembled where overlap was sufficient using the CAP3 web server (http://doua.prabi.fr/software/cap3).

Community iTag sequencing, operational taxonomic units, and single nucleotide variants

Sequentially filtered (2.7µm, 0.22µm) duplicate samples were extracted and analyzed using our previously reported protocols and settings (35, 68). We sequenced the 2.7-0.22 µm fraction for this study because this fraction corresponded with the < 2.7 µm communities that were used for the DTE experiments. To avoid batch sequencing effects, DNA from the first seven collections reported in (35) was resequenced with the additional samples from this study (FWC2 and after-Table 1). We targeted the 16S rRNA gene V4 region with the 515F, 806RB primer set (that corrects for poor amplification of taxa like SAR11) (69, 70) using Illumina MiSeq 2 x 250bp paired-end sequencing at Argonne National Laboratories, resulting in 2,343,106 raw reads for the 2.7-0.22 µm fraction. Using Mothur v1.33.3 (71), we clustered 16S rRNA gene amplicons into distinctive OTUs with a 0.03 dissimilarity threshold ($OTU_{0.03}$) and classified them according to the Silva v119 database (72, 73). After these steps, 55,256 distinct $OTUs_{0.03}$ remained. We also used minimum entropy decomposition (MED) to partition reads into fine-scale amplicon single nucleotide variants (ASVs) (74). Reads were first analyzed using Mothur as described above up to the *screen.seqs()* command. The cleaned reads fasta file was converted to MED-compatible headers with the 'mothur2oligo' tool renamer.pl from the functions in MicrobeMiseq (https://github.com/DenefLab/MicrobeMiseq) (75) using the fasta output from *screen.seqs()* and

the Mothur group file. These curated reads were analyzed using MED (v. 2.1) with the flags –M 60, and -d 1. MED resulted in 2,813 refined ASVs. ASVs were classified in Mothur using *classify.seqs()*, the Silva v119 database, and a cutoff bootstrap value of 80% (76). After classification, we removed ASVs identified as "chloroplast", "mitochondria", or "unknown" from the dataset.

Community analyses

OTU ($OTU_{0.03}$) and ASV abundances were analyzed within the R statistical environment v.3.2.1 (77) following previously published protocols (29, 35, 68). Using the package PhyloSeq (78), OTUs and ASVs were rarefied using the command *rarefy_even_depth()* and OTUs/ASVs without at least two reads in four of the 34 samples (2 sites; ~11%) were removed. This latter cutoff was used to remove potentially spurious OTUs/ASVs resulting from sequencing errors. Our modified PhyloSeq scripts are available on our GitHub repository https://github.com/thrash-lab/Modified-Phyloseq. After filtering, the datasets contained 777 unique OTUs and 1,323 unique ASVs (Table S1). For site-specific community comparisons, beta diversity between sites was examined using Bray-Curtis distances via ordination with non-metric multidimensional scaling (NMDS) (Table S1). The nutrient data were normalized using the R function *scale* which subtracts the mean and divides by the standard deviation for each column. The influence of the transformed environmental parameters on beta diversity was calculated in R with the *envfit* function. Relative abundances of an OTU or ASV from each sample were calculated as the number of reads over the sum of all the reads in that sample. The relative abundance was then averaged between biological duplicates for a given OTU or ASV. To determine the best matching OTU or ASV for a given LSUCC isolate, the OTU representative fasta file, provided by Mothur using *get.oturep*(), and the ASV fasta file were used to create a BLAST database (*makeblastdb*) against which the LSUCC isolate 16S rRNA genes could be searched via blastn (BLAST v 2.2.26) ("OTU_ASVrep_db" - Available as Supplemental Information at https://doi.org/10.6084/m9.figshare.12142098). We designated a LSUCC isolate 16S rRNA gene match with an OTU or ASV sequence based on ≥ 97% or ≥ 99% sequence identity, respectively, as well as a ≥ 247 bp alignment.

16S rRNA gene phylogeny

Taxa in the *Alpha-*, *Beta-*, and *Gammaproteobacteria* phylogenies from (35) served as the backbone for the trees in the current work. For places in these trees with poor representation near isolate sequences, additional taxa were selected by searching the 16S rRNA genes of LSUCC isolates against the NCBI nt database online with BLASTn (79) and selecting a variable number of best hits. The *Bacteroidetes* and *Actinobacteria* trees were composed entirely of non-redundant top 100-300 MegaBLAST hits to a local version of the NCBI nt database, accessed August 2018. Sequences were aligned with MUSCLE v3.6 (80) using default settings, culled with TrimAl v1.4.rev22 (81) using the -automated1 flag, and the final alignment was inferred with IQ-TREE v1.6.11 (82) with default settings and -bb 1000 for ultrafast bootstrapping (83). Tips were edited with the nw_rename script within Newick Utilities v1.6 (84) and trees were visualized with Archaeopteryx (85). Fasta files for these trees and the naming keys are available as Supplemental Information at https://doi.org/10.6084/m9.figshare.12142098.

Assessment of isolate novelty

We quantified taxonomic novelty using BLASTn of our isolate 16S rRNA genes to those of other known isolates collected in three databases: 1) The NCBI nt database (accessed August 2018) - "NCBIdb"; 2) a custom database comprised of sequences from DTE experiments in other labs - "DTEdb"; and 3) a database containing all of our isolate 16S rRNA genes - "LSUCCdb". The DTEdb and LSUCCdb fasta files are available as Supplemental Information at https://doi.org/10.6084/m9.figshare.12142098. We compared our isolate sequences to these databases as follows:

1) All representative sequences were searched against the nt database using BLASTn (BLAST+v. 2.7.1) with the flags -perc_identity 84, -evalue 1E-6, -task blastn, -outfmt "6 qseqid sseqid pident length slen qlen mismatch evalue bitscore sscinames sblastnames stitle", and -negative_gilist to remove uncultured and environmental sequences. The negative GI list was obtained by searching `"environmental samples"[organism] OR metagenomes[orgn]"` in the NCBI Nucleotide database (accessed September 12th, 2018) and hits were downloaded in GI list format. This negative GI list is available as Supplemental Information at https://doi.org/10.6084/m9.figshare.12142098. The resultant hits from the NCBIdb search were further manually curated to remove sequences classified as single cell genomes, clones, duplicates, and previously deposited LSUCC isolates.
2) We observed that many known HTCC, IMCC, and HIMB isolates that had previously been described as matching our clades (Figs. S1-5) were missing from the resultant lists of nt hits, so we extracted isolate accession numbers from numerous DTE experiments (26–28, 31, 34, 37, 44, 86, 87) from the nt database via *blastdbcmd* and generated a separate DTEdb using *makeblastdb*. Duplicate accession numbers found in the NCBIdb were removed. The same BLASTn settings as in 1) were used to search our isolate sequences against DTEdb. Any match that fell below the lowest percent identity hit to the NCBIdb was removed from the DTEdb search since the match would not have been present in the first NCBIdb search.
3) Finally, using the same BLASTn settings, we compared all pairwise identities of our 328 LSUCC isolate 16S rRNA gene sequences via the LSUCCdb.

The output from these searches is available in Table S1 under the "taxonomic novelty" tab.

We placed our LSUCC isolates into 55 taxonomic groups based on sharing ≥ 94% identity and/or their occurrence in monophyletic groups within our 16S rRNA gene trees (Figs. S1-5, see above). For visualization purposes, in groups with multiple isolates we used our chronologically first cultivated isolate as the representative sequence for blastn searches, and these are the top point (100% identity to itself) in each group column of Figure 1. Sequences from the other DTE culture collections were labeled with the corresponding collection name, while all other hits were labeled as "Other".

Geographic novelty was assessed by manually screening the accession numbers from hits to LSUCC isolates with ≥ 99% 16S rRNA gene sequence identity for the latitude and longitude from a connected publication or location name (e.g. source, country, site) in the NCBI description. LSUCC isolates in the *Janibacter* sp., *Micrococcus* sp., *Altererythrobacter* sp., *Pseudomonas* sp., and *Phycicoccus* sp. groups (16 total isolates) were not assessed because of missing isolation source information and no traceable publication. Isolation locations were plotted for a subset of important taxa (Table S1 "Map_cultivars" tab) using the "LSUCC_cultivar_map.R" available at our GitHub repository https://github.com/thrash-lab/Cultivar-novelty-map.

Modeling DTE cultivation via Monte Carlo simulations

We developed a model using Monte Carlo simulation to estimate the median number of positive and pure wells (and associated 95% confidence intervals (CI)) expected from a DTE experiment for a given taxon at different inoculum sizes (λ), relative abundances (r), and viability (V) (Fig. 5). For each bootstrap, the number of cells added to each well was simulated using a Poisson distribution at a mean inoculum size of λ cells per well across n wells. The number of cells added to each well that belonged to a specific taxon was then estimated using a binomial distribution where the number of trials was set as the number of cells in a well and the probability of a cell belonging to a specific taxon, r, was the relative abundance of its representative ASV in the community analysis. Wells that contained at least one cell of a specific taxon were designated 'positive'. Wells in which all the cells belonged to a specific taxon were designated as 'pure'. Finally, the influence of taxon-specific viability on recovery of 'pure' wells was simulated using a second binomial distribution, where the number of cells within a 'pure' well was used as the number of trials and the probability of growth was a viability score ranging from 0 to 1. For each simulation, 9,999 bootstraps were performed. Code for the model and all simulations is available in the 'viability_test.py' at our GitHub repository https://github.com/thrash-lab/viability_test.

Actual versus expected number of isolates

For each taxon in each DTE experiment, the Monte Carlo simulation was used to evaluate whether the number of recovered pure wells for each taxon was within 95% CI of simulated estimates, assuming optimum growth conditions (i.e. V = 100%). For each of 9,999 bootstraps, 460 wells were simulated with the inoculum size used for the experiment and the relative abundance of the ASV. For taxa where the number of expected wells fell outside the 95% CI of the model, a deviance score was calculated as the difference between the actual number of wells observed and median of the simulated dataset. The results of this output are presented in Table S1 under the "Expected vs actual" tab, and the R script for visualizing this output as Figure 7 is available at our GitHub repository https://github.com/thrash-lab/EvsA-visualization.

Estimating viability in under-represented taxa

For taxa where the observed number of positive wells was lower than the 95% CI lower limit within a given experiment, and because our analysis was restricted to only those organisms for which our media was sufficient for growth at least once, the deviance was assumed to be a function of a viability term, V, (ranging from 0 to 1) associated with suboptimal growth conditions, dormancy, persister cells, etc. To estimate a value of viability for a given taxon within a particular experiment, the Monte Carlo simulation was run using an experiment-appropriate inoculum size, relative abundance, and number of wells (460 for each experiment). Taxon-specific viability was tested across a range of decreasing values from 99% to 1% until such time as the observed number of pure wells for a given taxon fell between the 95% CI bounds of the simulated data. At this point, the viability value is the maximum viability of the taxon that enables the observed number of pure wells for a given taxon to be explained by the model. The results of this output are presented in Table S1 under the "Expected vs actual" tab.

Likelihood of recovering taxa at different relative abundances

To estimate the number of wells required in a DTE experiment to have a significant chance of recovering a taxon with a relative abundance of r, assuming optimum growth conditions (V =

100%), the Monte Carlo model was used to simulate experiments from 92 wells to 9,200 wells per experiment across a range of relative abundances from 0 to 100% in 0.1% increments, and a range of inoculum sizes (cells per well of 1, 1.27, 1.96, 2, 3, 4 and 5). Each experiment was bootstrapped 999 times and the number of bootstraps in which the lower-bound of the 95% CI was ≥ 1 was recorded.

Data accessibility

All iTag sequences are available at the Short Read Archive with accession numbers SRR6235382-SRR6235415 (29). PCR-generated 16S rRNA gene sequences from this study are accessible on NCBI GenBank under the accession numbers MK603525-MK603769. Previously generated 16S rRNA genes sequences are accessible on NCBI GenBank under the accession numbers KU382357-KU38243 (35). Table S1 is available at https://doi.org/10.6084/m9.figshare.12142113.

Results

General cultivation campaign results

We conducted a total of seventeen DTE cultivation experiments to isolate bacterioplankton (sub 2.7 µm fraction), with paired microbial community characterization of source waters (0.22 µm - 2.7 µm fraction), from six coastal Louisiana sites over a three-year period (Table S1). We inoculated 7,820 distinct cultivation wells (all experiments) with an estimated 1-3 cells·well^{-1} using overlapping suites of artificial seawater media, JW (years 1 and 2, (35)) and MWH (year 3), designed to match the natural environment (Table 1). The MWH suite of media was modified from the JW media to additionally include choline, glycerol, glycine betaine, cyanate, DMSO, DMSP, thiosulfate, and orthophosphate (Table S1). These compounds have been identified as important metabolites and osmolytes for marine and freshwater microorganisms and were absent in the first iteration (JW) of our media (88–94). A total of 1,463 wells were positive (> 10^4 cells·ml^{-1}), and 738 of these were transferred to 125 mL polycarbonate flasks. For four experiments (FWC, FWC2, JLB2, and JLB3) we only transferred a subset of positives (48/301, 60/403, 60/103, and 60/146) because the number of isolates exceeded our ability to maintain and identify them at that time (Table 1). The subset of positive wells for these four experiments was selected using flow cytometry signatures usually indicative of smaller oligotrophic cells like SAR11 strain HTCC1062 (49) using our settings. Of the 738 wells from which we transferred cells across all experiments, 328 of these yielded repeatably transferable isolates that we deemed as pure cultures based on 16S rRNA gene PCR and Sanger sequencing.

Table 1. Cultivation statistics, including whole community viability estimates

Site	Date	*n*	*z*	*p*	*λ*	*V** (ASE)	CV	our model: estimated # wells with 1 cell (bootstrapped median: (xx-xx) 95% CI) if *V*==1 **	our model: V_{est}: min-max 95% CI ***	*in situ* salinity	Medium salinity	Medium	Study
CJ	Sep 2014	460	15	0.033	1.27	2.6 (0.67)	0.259	164 (144-185)	1.5-4.2	24.6	34.8	JWAMPFe	(35)
ARD	Nov 2014	460	1	0.002	1.5	0.1 (0.15)	1.451	154 (134-174)	0.1-0.7	1.72	34.8	JW1	(35)
JLB	Jan 2015	460	61	0.133	1.96	7.3 (0.93)	0.127	127 (109-146)	5.6-9.2	26.0	34.8	JW1	(35)
FWC†	Mar 2015	460	301	0.654	2	53.1 (3.2)	0.06	125 (106-143)	47.1-59.7	5.39	5.79	JW4	(35)
LKB	June 2015	460	15	0.033	1.8	1.8 (0.48)	0.266	137 (118-156)	1.1-3.0	2.87	5.79	JW4	(35)
Tbon2	Aug 2015	460	41	0.089	1.56	6.0 (0.93)	0.156	151 (132-171)	4.3-8.1	14.2	11.6	JW3	(35)

CJ2	Oct 2015	460	61	0.133	2	7.1 (0.91)	0.128	125 (106-143)	5.6-9.1	22.2	23.2	JW2	(35)
FWC2†	Apr 2016	460	403	0.876	2	104.4 (6.2)	0.059	125 (106-143)	>92.3	20.9	23.2	JW2	This study
ARD2c	Jun 2016	460	7	0.015	2	0.8 (0.29)	0.362	125 (106-143)	0.3-1.5	0.18	1.45	JW5	This study
JLB2c†	May 2016	460	103	0.224	2	12.7 (1.25)	0.099	125 (106-143)	10.3-15.4	6.89	5.79	JW4	This study
LKB2	Jul 2016	460	39	0.085	2	4.4 (0.71)	0.161	125 (106-143)	3.2-6.0	2.39	1.45	JW5	This study
Tbon3	Jul 2016	460	78	0.17	2	9.3 (1.05)	0.113	125 (106-143)	7.4-11.5	17.7	34.8	MWH1	This study
CJ3	Sep 2016	460	69	0.15	2	8.1 (0.98)	0.121	125 (106-143)	6.4-10.2	23.7	23.2	MWH2	This study
FWC3	Nov 2016	460	27	0.059	2	3.0 (0.58)	0.194	125 (106-143)	2.0-4.4	18.0	23.2	MWH2	This study
ARD3	Dec 2016	460	58	0.126	2	6.7 (0.89)	0.132	125 (106-143)	5.2-8.6	3.72	1.45	MWH5	This study
JLB3†	Jan 2017	460	146	0.317	2	19.1 (1.59)	0.083	125 (106-143)	16.1-22.4	12.4	11.6	MWH3	This study
LKB3	Feb 2017	460	38	0.083	2	4.3 (0.70)	0.163	125 (106-143)	3.1-5.8	3.55	1.45	MWH5	This study

*Viability according to equation 1, below. Asymptotic Standard Error (ASE) is presented in parentheses.
**Based on 9,999 bootstraps.
***Based on 9,999 bootstraps tested at viability increments of 0.1%.
†Experiments where a subset of positive wells were transferred.
FWC2 shows the advantage of our method over equation 1 for extreme values.

Phylogenetic and geographic novelty of our isolates

The 328 isolates belonged to three Phyla: *Proteobacteria* (n = 319), *Actinobacteria* (n = 8), and *Bacteroidetes* (n = 1) (Figs. S1-S5). We placed these isolates into 55 groups based on their positions within 16S rRNA gene phylogenetic trees (Figs. S1-S5) and as a result of having ≥ 94% 16S rRNA gene sequence identity to other isolates. We applied a nomenclature to each group based on previous 16S rRNA gene database designations and/or other cultured representatives (Fig. 1, Table S1). Isolates represented eight putatively novel genera with ≤ 94.5% 16S rRNA gene identity to a previously cultured representative: the *Actinobacteria* acIV subclades A and B, and one other unnamed *Actinobacteria* group; an undescribed *Acetobacteraceae* clade (*Alphaproteobacteria*); the freshwater SAR11 LD12 (*Candidatus* Fonsibacter ubiquis (29)); the MWH-UniPo and an unnamed *Burkholderaceae* clade (*Betaproteobacteria*); and the OM241 *Gammaproteobacteria* (Fig. 1, Table S1). Seven additional putatively novel species in other genera were also isolated (between 94.6 and 96.9% 16S rRNA gene sequence identity) in unnamed *Commamonadaceae* and *Burkholderiales* clades (*Betaproteobacteria*); the SAR92 clade and *Pseudohonigella* genus (*Gammaproteobacteria*); and unnamed *Rhodobacteraceae* and *Bradyrhizobiaceae* clades, as well as *Maricaulis* spp. (*Alphaproteobacteria*) (Fig. 1). LSUCC isolates belonging to the groups BAL58 *Betaproteobacteria* (Fig. S4), OM252 *Gammaproteobacteria*, HIMB59 *Alphaproteobacteria*, and what we designated the LSUCC0101-type *Gammaproteobacteria* (Fig. S5) had close 16S rRNA gene matches to other isolates at the species level, however, none of those previously cultivated organisms have been formally described (Fig. 1). The OM252, BAL58, and MWH-UniPo clades were the most frequently cultivated, with 124 of our 328 isolates belonging to these three groups (Table S1). In total, 73 and 10 of the 328 isolates belonged in putatively novel genera and novel species in previously cultivated genera, respectively. We estimated that at least 310 of these isolates were geographically novel, being the first of their type cultivated from the nGOM (Fig. 2). This included isolates from cosmopolitan groups like SAR11 subclade IIIa, OM43 *Betaproteobacteria*, SAR116, and HIMB11-type "Roseobacter" spp. Cultivars from *Vibrio sp.* and *Alteromonas sp.* were the only two groups with close relatives (species level) isolated from the GOM.

Natural abundance of isolates

We matched LSUCC isolate 16S rRNA gene sequences with both operational taxonomic units (OTUs) and amplicon single nucleotide variants (ASVs) from bacterioplankton communities to

assess the relative abundances of our isolates in the coastal nGOM waters that served as inocula. While OTUs provide a broad group-level designation (97% sequence identity), this approach can artificially combine multiple ecologically distinct taxa (95). Due to higher stringency for defining a matching 16S rRNA gene, ASVs can increase the confidence that our isolates represent environmentally relevant organisms (74, 96). However, while many abundant oligotrophic bacterioplankton clades such as SAR11 (29, 97), OM43 (40, 41), SAR116 (98), and *Sphingomonas* spp. (99) have a single copy of the rRNA gene operon, other taxa can have multiple rRNA gene copies (97, 100), complicating ASV analyses. Since we could not *a priori* rule out multiple rRNA gene operons for novel groups with no genome sequenced representatives, we used both OTU and ASV approaches.

In total, we obtained at least one isolate from 40 of the 777 OTUs and 71 of the 1,323 ASVs observed throughout the three-year dataset. 43% and 26% of LSUCC isolates matched the top 50 most abundant OTUs (median relative abundances, all sites, from 8.1-0.11%; Fig. S6A) and ASVs (mean relative abundances, all sites, from 3.8-0.11%; Fig. S6B), respectively, across all sites and samples. Microbial communities from all collected samples clustered into two groups corresponding to those inhabiting salinities below 7 and above 12, and salinity was the primary environmental driver distinguishing community beta diversity (OTU: R^2=0.88, P=0.001, ASV: R^2=0.89, P =0.001). As part of the cultivation strategy after the first five experiments, we used a suite of five media differing by salinity and matched the experiment with the medium that most closely resembled the salinity at the sample site. Consequently, our isolates matched abundant environmental groups from both high and low salinity regimes. At salinities above twelve, LSUCC isolates matched 13 and 14 of the 50 most abundant OTUs and ASVs, respectively (Figs. 3A, 4A; Table S1). These taxa included the abundant SAR11 subclade IIIa.1, HIMB59, HIMB11-type "Roseobacter", and SAR116 *Alphaproteobacteria*; the OM43 *Betaproteobacteria*; and the OM182 and LSUCC0101-type *Gammaproteobacteria*. At salinities below seven, 10 and 9 of the 50 most abundant OTUs and ASVs, respectively, were represented by LSUCC isolates, including one of most abundant taxa in both cluster sets, SAR11 LD12 (Figs. 3B, 4B). Some taxa, such as SAR11 IIIa.1 and OM43, were among the top 15 most abundant taxa in both salinity regimes (Figs. 3, 4, Table S1), suggesting a euryhaline lifestyle. In fact, our cultured SAR11 IIIa.1 ASV7471 was the most abundant ASV in the aggregate dataset (Fig. S6).

Overall, this effort isolated taxa representing 18 and 12 of the top 50 most abundant OTUs and ASVs, respectively (Table 2, Fig. S6). When looking at different median relative abundance categories of > 1%, 0.1% - 1%, and < 0.1%, isolate OTUs were distributed across those categories in the following percentages: 15%, 20%, and 27%; isolate ASVs were distributed accordingly: 4%, 26%, and 37% (Table 2). Isolates with median relative abundances of < 0.1%, such as *Pseudohongiella* spp., *Rhodobacter* spp., and *Bordetella* spp., would canonically fall within the rare biosphere (101) (Table S1). A number of isolates did not match any identified OTUs or ASVs (38% and 33% of LSUCC isolates when compared to available OTUs and ASVs, respectively), either because their matching OTUs/ASVs were below our thresholds for inclusion (at least two reads from at least two sites), or because they were below the detection limit from our sequencing effort (Table 2). Thus, 43% and 30% of our isolates belonged to OTUs and ASVs, respectively, with median relative abundances > 0.1%.

Table 2. Median relative abundances (*r*) of cultured OTUs and ASVs across all samples

	In top 50 ranks	*r* > 1%	1% - 0.1% *r*	*r* < 0.1%	Not detected
OTUs	18 (140 isolates)	50 isolates (15%)	90 isolates (27%)	65 isolates (20%)	123 isolates (38%)

ASVs	12 (84 isolates)	13 isolates (4%)	84 isolates (26%)	122 isolates (37%)	109 isolates (33%)

Modeling DTE cultivation

An enigma that became immediately apparent through a review of our data was the absence of an obvious relationship between the abundance of a given taxon in the inoculum and the frequency of obtaining an isolate of the same type from a DTE cultivation experiment (Figs. S7, S8). For example, although we could culture SAR11 LD12 over a range of media conditions (29), and the matching ASV had relative abundances of > 5% in six of our seventeen experiments (Fig. 5), we only isolated one representative (LSUCC0530). In an ideal DTE cultivation experiment where cells are randomly subsampled from a Poisson-distributed population, if the medium is sufficient for a given microorganism's growth, then the number of isolates should correlate with that microorganism's abundance in the inoculum. However, a qualitative examination of several abundant taxa that grew in our media, some of which we cultured on multiple occasions, revealed no clear pattern between abundance and isolation success (Fig. 5). Considering that medium composition was sufficient for cultivation of these organisms on at least some occasions, we hypothesized that cultivation frequency may reflect differences in the capacity for growth within populations of a given taxon. Thus, we decided to model cultivation frequency in relationship to estimated abundances in a way that could generate estimates of cellular viability, defined herein as meaning "presently able to grow in defined medium," as opposed to a broader definition equating viability with being alive more generally, since we only evaluated growth capacity in this study. We hoped that modeling might also help us inform experimental design and make DTE cultivation efforts more predictable (59).

Previously, Don Button and colleagues developed a statistical model for viability (V) of cells in the entire population for a DTE experiment (33):

$$(1)\ V = -\frac{\ln(1-p)}{\lambda}$$

Where p is the proportion of wells or tubes, n, with growth, z, $(p = z/n)$ and λ is the estimated number of cells inoculated per well (the authors used X originally). The equation uses a Poisson distribution to account for the variability in cell distribution within the inoculum and therefore the variability in the number of wells or tubes receiving the expected number of cells. We and others have used this equation in the past (26, 28, 35) to evaluate the efficacy of our cultivation experiments in the context of commonly cited numbers for cultivability using agar-plate based methods (13, 17, 102).

While Equation 1 was effective for its intended purpose, it has a number of drawbacks that limit its utility for taxon-specific application: 1) If $p=1$, i.e. all wells are positive, then the equation is invalid; 2) At high values of p and low values of λ, estimates of V can exceed 100% (Table 1); 3) Accuracy of viability, calculated by the asymptotic standard error, *ASE*, or the coefficient of variation, *CVV*, was shown to be non-uniform across a range of λ, with greatest accuracy when true viability was ~10% (33). Thus, low viability, low values of λ, and small values of n were found to produce unreliable results; 4) If $p=0$, i.e. no positive wells are observed, estimates of viability that could produce 0 positive wells cannot be calculated. In addition, 5) Button's original model assumes that a well will only produce a pure culture if the inoculated well contains one cell. By contrast, in low diversity samples, samples dominated by a single taxon, or experiments evaluating viability from axenic cultures across different media, a

limitation that only wells with single cells are axenic will underestimate the expected number of pure wells.

To overcome these limitations, we developed a Monte Carlo simulation model that facilitates the incorporation of relative abundance data from complementary community profiling data (e.g. 16S rRNA gene amplicons) to calculate the likelihood of positive wells, pure wells, and viability at a taxon-specific level, based on the observed number of wells for which we obtained an isolate of a particular taxon (Fig. 6). By employing a Monte Carlo approach, our model is robust across all values of p and n with uniform prediction accuracy, and we can estimate the accuracy of our prediction within 95% confidence intervals (CI). Furthermore, the width of 95% CI boundaries of viability, as well as the expected number of positive and pure wells, are entirely controllable and dependent only on available computational capacity for bootstrapping (i.e., these can be improved with more bootstrapping, but at greater computational cost). When zero positive wells are observed experimentally, our approach enables estimation of a maximum viability that could explain such an observation by identifying the range of variability values for which zero resides within the bootstrapped 95% CI. Finally, the ability to calculate the viability of the entire community, as in Equation 1, is retained simply by estimating viability using a relative abundance of one.

We compared our model to that of Button et al. for evaluating viability from whole community experimental results, similarly to previous reports (26, 28, 35) (Table 1). Our viability estimates (V_{est}) generally agreed with those using the Button et al. calculation, but we have now provided 95% CI to depict the maximum and minimum viability that would match the returned positive well distribution, as well as maximum and minimum values for the number of wells that ought to have contained a single cell. Maximum V_{est} ranged from 1.1% to > 92.3% depending on the experiment, with a median V_{est} across all our experiments of 8.6% (Table 1). In one case, the extremely high value (FWC2) was better handled by our model compared to equation 1, because it did not lead to a viability estimation greater than 100%. FWC and FWC2 represent V_{est} outliers compared with the entire dataset (maximums of 59.7% and > 92.3%, respectively; Table 1). We believe these high numbers most likely resulted from underestimating the number of cells inoculated into each well (because of the use of microscopy, the presence of clumped cells, or possible pipet error- described in (35)), thus increasing the estimated viability.

Isolate-specific viability estimates

Our new model also facilitates taxon-specific viability estimates. Cultivation efficacy was evaluated for 71 cultured taxa matching ASVs within our detection limits (219 isolates) across 17 sites (1,207 pairwise combinations) by comparing the number of observed pure wells to those predicted by the Monte Carlo simulation using 9,999 bootstraps, 460 wells per experiment, and an assumption that all cells were viable (i.e. V = 100%). In total, for 1,158 out of 1,207 pairwise combinations (95.9%) the observed number of pure wells fell within the 95% CI of data simulated at matching relative abundance and inoculum size, suggesting that these two parameters alone could explain the observed cultivation success for most taxa (Table S1). 1,059 out of these 1,158 combinations (91%) recorded zero observed wells, but with a maximum relative abundance of 2.8% within these combinations, a score of zero fell within predicted 95% CI of simulations with 460 wells. Sensitivity analysis showed that with 460 wells per experiment, an observation of zero pure wells falls below the 95% confidence intervals lower-bound (and is thus significantly depleted to enable viability to be estimated) for taxa with relative abundances of 2.3%, 2.9% and 4.5% for inoculum sizes of one, two and three cells per well,

respectively (Fig. S9). In fact, modeling DTE experiments from 92 wells to 9,200 wells per experiment showed that for taxa comprising ~1% of a microbial community 1,104 wells (or 12 plates at 92 wells per plate), 1,380 wells (15 plates) and 2,576 wells (28 plates) were required to be statistically likely to recover at least one positive, pure well using inocula of one, two or three cells per well, respectively, with V = 100% (Fig. S9).

A small, but taxonomically relevant minority (49 out of 1,207) of pairwise combinations had a number of observed pure wells that fell outside of the simulated 95% CI with V = 100% (Fig. 7). Of these, 28 had either one, two, or three more observed pure wells than the upper 95% CI (Table S1), suggesting cultivability *higher* than expected based purely a model capturing the interaction between a Poisson-distributed inoculum and a binomially-distributed relative abundance, with V = 100%. However, the deviance from the expected number of positive wells for those above the 95% CI was limited to three or fewer wells, meaning that we only obtained 1-3 more isolates than expected (Table S1). On the other hand, those organisms that we isolated less frequently than expected showed greater deviance. 21 out of the 49 outliers had lower than expected cultivability (Fig. 7). These taxa had relative abundances ranging from 2.7% to 14.5%, but recorded only 0, 1, or 2 isolates. In the most extreme case, ASV7629 (SAR11 LD12) at Site ARD2c comprised 14.5% of the community but recorded no observed pure wells, compared to expected number of 13-30 isolates (95% CI) predicted by the Monte Carlo simulation. All the examples of taxa that were isolated less frequently than expected given the assumption of V = 100% belonged to either SAR11 LD12, SAR11 IIIa.1, or one particular OM43 ASV (7241) (Fig. 6).

We used our model to calculate estimated viability (V_{est}) for these organisms based on their cultivation frequency at sites where the assumption of V = 100% appeared violated (Table 3). Using the extreme example of SAR11 LD12 ASV7629 at Site ARD2c, simulations across a range of V indicated that a result of zero positive wells fell within 95% of simulated values when the associated taxon $V_{est} \leq 15\%$. When considering all anomalous cultivation results, LD12 had estimated maximum viabilities that ranged up to 55% (Table 3). OM43 (ASV7241) estimated maximum viabilities ranged from 52-80%, depending on the site, and similarly, SAR11 IIIa.1 ranged between 22-82% maximum viability (Table 3).

Table 3. Estimated viabilities for taxa cultivated less frequently than expected

ASV	Group	Site	r*	n	z	λ	Estimated # wells with 1 cell (bootstrapped median: (xx-xx) 95% CI) if V==1 **	V_{est}: min-max 95% CI based on cultivation results***
7241	OM43	ARD3	0.03	460	0	2	4 (1-9)	0.1-80
7241	OM43	FWC†	0.04	460	0	2	5 (1-9)	0.1-77
7241	OM43	JLB	0.05	460	0	1.96	7 (2-12)	0.1-52
7471	SAR11 IIIa.1	ARD3	0.11	460	0	2	15 (8-23)	0.1-22
7471	SAR11 IIIa.1	CJ	0.03	460	0	1.27	4 (1-9)	0.1-82
7471	SAR11 IIIa.1	FWC3	0.07	460	2	2	9 (4-15)	2.5-80
7471	SAR11 IIIa.1	JLB	0.05	460	0	1.96	6 (2-11)	0.1-59
7471	SAR11 IIIa.1	JLB2c†	0.08	460	0	2	11 (5-18)	0.1-31
7471	SAR11 IIIa.1	JLB3†	0.04	460	0	2	5 (1-9)	0.1-74
7471	SAR11 IIIa.1	LKB	0.05	460	0	1.8	6 (2-12)	0.1-55
7471	SAR11 IIIa.1	LKB2	0.04	460	0	2	5 (1-9)	0.1-77
7471	SAR11 IIIa.1	LKB3	0.09	460	0	2	11 (6-19)	0.1-30
7471	SAR11 IIIa.1	TBON2	0.04	460	0	1.56	6 (2-12)	0.1-56
7471	SAR11 IIIa.1	TBON3	0.04	460	0	2	5 (1-10)	0.1-73
7629	SAR11 LD12	ARD	0.11	460	0	1.5	18 (10-27)	0.1-20
7629	SAR11 LD12	ARD2c	0.15	460	0	2	21 (13-30)	0.1-15
7629	SAR11 LD12	ARD3	0.05	460	0	2	7 (2-12)	0.1-53
7629	SAR11 LD12	FWC†	0.09	460	0	2	12 (6-19)	0.1-28

7629	SAR11 LD12	LKB	0.05	460	0	1.8	7 (2-13)	0.1-51
7629	SAR11 LD12	LKB2	0.08	460	1	2	11 (5-18)	0.3-49
7629	SAR11 LD12	LKB3	0.06	460	0	2	7 (3-13)	0.1-48

*Fractional relative abundance
**Based on 9,999 bootstraps.
***Based on 9,999 bootstraps tested at viability increments of 0.1%.
†Experiments where a subset of positive wells were transferred.

Discussion

This work paired 17 DTE cultivation experiments with cultivation-independent assessments of microbial community structure in source waters to evaluate cultivation efficacy. We generated 328 new bacterial isolates representing 40 of the 777 OTUs and 71 of the 1,323 ASVs observed across all samples from which we inoculated DTE experiments. Stated another way, we successfully cultivated 5% of the total three year bacterioplankton community observed via either OTU or ASV analyses. A large fraction of our isolates (43% of cultured OTUs, 30% of cultured ASVs) represented taxa present at median relative abundances > 0.1%, with 15% and 4% of cultured OTUs and ASVs, respectively, at median abundances > 1%. 140 of our isolates matched the top 50 most abundant OTUs, and 84 isolates matched the top 50 most abundant ASVs.

This campaign led to the first isolations of the abundant SAR11 LD12 and *Actinobacteria* acIV; the second isolate of the HIMB59 *Alphaproteobacteria*; and new genera within the *Acetobacteraceae*, *Burkholderiaceae*, OM241 and LSUCC0101-type *Gammaproteobacteria*, and MWH-UniPo *Betaproteobacteria*; thereby demonstrating again that continued DTE experimentation leads to isolation of previously uncultured organisms with value for aquatic microbiology. We have also added a considerable collection of isolates to previously cultured groups like OM252 *Gammaproteobacteria*, BAL58 *Betaproteobacteria*, and HIMB11-type "Roseobacter" spp., and the majority of our isolates represent the first versions of these types of taxa from the Gulf of Mexico, adding comparative biogeographic value to these cultures.

Our viability model improved upon the statistical equation developed by Button and colleagues (33) to extend viability estimates to individual taxa within a mixed community and provide 95% CI constraining those viability estimates. We cultured several groups of organisms abundant enough to evaluate viability with 460 wells (Figs. 7, S9). The fact that these organisms were successfully cultured at least once meant that we could reasonably assume that the medium was sufficient for growth. Some taxa were cultivated more frequently than expected (Fig. 7). We explore two possible explanations for this phenomenon- errors in quantification and variation in microbial cell organization. Any systematic error that led to underestimating the abundance of an organism would have correspondingly resulted in our underestimating the number of wells in which we would expect to find a pure culture of that organism. Such underestimations could come from primer biases associated with amplicon sequencing (69, 70, 103), but we do not know if those protocols specifically underestimate the OM252, MWH-UniPo, and HIMB11-type taxa cultured more frequently than expected (Fig. 7). However, due the low number of expected isolates in these groups, and the small deviances in actual isolates from those expected numbers (within 1-3 isolates compared to expected values), the biases inherent in the relative abundance estimations for these taxa were probably small. Furthermore, one of the microorganisms isolated more frequently than expected matched the OM43 ASV1389 (Fig. S6), whereas another OM43 ASV (7241) was cultivated less frequently than expected (see below), meaning that if primer bias were the cause of this discrepancy, it would have to be operating differently on very closely related organisms.

One possible biological explanation for why some isolates might have been cultured more frequently than expected is clumped cells. If cells of any given taxon in nature grew in small clusters, then the number of cells we added to a well would have been greater than expected based on a Poisson distribution. Furthermore, the model assumes that each cell is independent, and that the composition of a subset of cells is only a function of the relative abundance of the taxon in the community. Within a cluster of cells, this assumption is violated as the probability of cells being from the same taxon is higher. Thus, the model will underestimate the probability of a well being pure and therefore underestimate the number of pure wells likely to be observed within an experiment, leading to a greater number of isolates than expected. Future microscopy work could examine whether microorganisms such as OM252 and MWH-UniPo form small clusters *in situ* and/or in pure culture, and whether this phenomenon may be different for different ASVs of OM43, or if clumping may be a transient phenotype.

We also identified three taxa- SAR11 LD12, SAR11 subclade IIIa.1, and the aforementioned OM43 ASV7241- that were isolated much less frequently than expected based on their abundances (Fig. 7, Table 3). This could mean that our assumption of $V = 100\%$ was incorrect, or that, in contrast to the taxa that were cultured more frequently than expected (above), our methods had biases that *over*estimated the abundance of these organisms, thereby over-inflating the expected number of isolates. We used the modified 515/806RB primers that have been shown to be much more accurate in quantifying SAR11 compared to FISH than the original 515/806 primers (within 6% ± 4% SD), and this protocol almost always underestimates SAR11 abundance (69). This suggests that our expected number of isolates may have actually been underestimated, our cultivation success poorer than we measured, and therefore we may be overestimating viability for the SAR11 taxa in this study. Other sources of systematic error that might impinge on successful transfers, and thereby reduce our recovery, include sensitivity to pipette tip and/or flask material. However, the fact that these taxa were sometimes successfully isolated means that if these mechanisms were impacting successful transfers, then their activity was less than 100% efficient, which implies variations in subpopulation vulnerability that would be very similar conceptually to variations in subpopulation viability.

Another possible source of error that could have resulted in lower than expected numbers of isolates was the subset of experiments for which we did not transfer all positive wells due to limitations in available personnel time (Tables 1 & 3). However, our selection criteria for the subset of wells to transfer was based on flow cytometric signatures that would have encompassed small cells like SAR11 (see Results), and in any case, there were many examples of lower than expected recovery from other experiments where we transferred all positive wells (Table 3). Thus, we believe that these four experiments were unlikely to contribute major errors biasing our estimates of viability for SAR11 LD12, SAR11 IIIa.1, and other small cells like OM43.

If we instead explore biological reasons for the lower than expected numbers of positive wells in DTE experiments, a plausible explanation supported by the literature is simply that a large fraction of the population is in some state of inactivity or at least not actively dividing (104). Studies using uptake of a variety of radiolabelled carbon and sulfur sources have demonstrated substantial fractions of SAR11 cells may be inactive depending on the population (105–108). SAR11 cells in the northwest Atlantic and Mediterranean showed variable uptake of labelled leucine (30-50% (105, 106); ~25-55% (108, 109)) and amino acids (34-61% (105, 106); 34-66% (105, 106)). Taken in reverse, this means that up to 75% of the SAR11 population may be dormant at any given time. In another study focused on brackish communities, less than 10% of SAR11 LD12 cells took up labelled leucine and/or thymidine (107). While this was likely not

the ideal habitat for LD12 based on salinities above six (29, 107), this study supports the others above that show substantial proportions of inactive SAR11 cells, the fraction of which may depend on environmental conditions and other unknown factors. Bi-orthagonal non-canonical amino acid tagging (BONCAT) shows similar trends for SAR11 (110). These results also match general data indicating prevalent inactivity among aquatic bacterioplankton (104, 111–113). Although labelled uptake methods do not directly measure rates of cell division, the incorporation of these compounds requires active DNA replication or translation, which represent an even more fundamental level of activity than cell division (114).

Why might selection favor high percentages of subpopulation dormancy? One possibility is as an effective defense mechanism against abundant viruses. Viruses infecting SAR11 have been shown to be extremely abundant in both marine (115, 116) and freshwater (117) systems. Indeed, the paradox of high viral abundances and high host abundances in SAR11 has led to a refining of negative density dependent selection through Lokta-Volterra predator-prey dynamics (118) to include heterogeneous susceptibility at the strain level (119, 120) and positive density dependent selection through intraspecific proliferation of defense mechanisms (121). Activity of lytic viruses infecting SAR11 *in situ* demonstrated that phages infecting SAR11 have lower ratios of viral transcripts to host cells compared to other abundant taxa, and that observed abrupt changes in these ratios suggest co-existence of several SAR11 strains with different life strategies and phage susceptibility (122). Phenotypic stochasticity of phage receptor expression has been shown to maintain a small proportion of phage-insensitive hosts within a population, enabling coexistence of predator and prey without extinction (123). Phages adsorb to a vast array of receptor proteins on their hosts, with many well-characterised receptors (e.g. OmpC, TonB, BtuB, LamB) associated with nutrient uptake or osmoregulation (124). Selection therefore favours phenotypes that limit receptor expression, with an associated fitness cost, particularly in nutrient-limited environments.

However, an alternative mechanism is possible if a population of cells comprised a small number of susceptible cells, and a large number of either resistant or dormant cells where presentation of receptor proteins is retained. The majority of host-virus encounters would occur with resistant or dormant cells, and constrain viral propagation through inefficient or failed infection, effectively acting as a sink for infectious particles. Prevalent lysogeny in SAR11 populations would provide a mechanism for establishing resistant cells via superinfection immunity (125, 126), where integration of a temperate phage prevents infection by other closely related viruses. There is growing evidence that many viruses infecting SAR11 are temperate (127, 128) and that reversion to virulence can be triggered through nutrient limitation (128) in contrast to other systems where lysogeny is favoured in nutrient-poor conditions (129). Viral infection may also trigger host dormancy, lowering cellular metabolism to minimise energy requirements under nutrient limited conditions (130). Such cells would be selected against during cultivation experiments, potentially explaining the rarity of SAR11 isolate genomes found to contain prophages. Dormancy and/or lysogeny would also enable long-term co-stability between abundant phages and their hosts (131) and resolve the apparent paradox of high host and virus abundances (126).

Detailed measurements of dormancy in SAR11 and what types of cellular functions become inactivated are part of our ongoing work. In the meantime, it is prudent to examine the implications of a substantial proportion of non-dividing cells for our understanding of basic growth dynamics. Studies attempting to measure SAR11 growth rates in nature have yielded a wide range of results, ranging from 0.03-1.8 day^{-1} (97, 105, 108, 132–134). These span wider

746 growth rates than observed for axenic cultures of SAR11 (0.4-1.2 day^{-1}), but isolate-specific
747 growth ranges within that spread are much more constrained (29, 36, 49, 135, 136). Conversion
748 factors for determining production from ^{3}H-leucine incorporation (137) are accurate for at least
749 some Ia subclade members of SAR11 (138), so variations in growth rate estimates from
750 microradiography experiments likely have other explanations. It is possible that different strains
751 of SAR11 simply have variations in growth rate not captured by existing isolates. Another, not
752 mutually exclusive, possibility is that the differences in *in situ* growth rate estimates also reflect
753 variations in the proportion of actively dividing cells within the population. A simple model of
754 cell division with binary fission where only a subset of cells divide and non-dividing cells
755 persist, rather than die, can still yield logarithmic growth curves (Fig. S10) like those observed
756 for SAR11 in pure culture (29, 49, 139). However, this subpopulation variability means that the
757 division rate for the subset of cells that are actively dividing is much higher than calculated when
758 assuming 100% dividing cells in the population. Based on our estimated viability for SAR11
759 LD12 of 15-55%, to obtain our previously calculated maximum division rate (0.5 day^{-1}) for the
760 whole culture (29), the per-cell division rate for only a subpopulation would span 2.48-0.79 day^{-1}
761 (Fig. S10, Supplemental Text). Verifying the proportion of SAR11 cells actively dividing in a
762 culture may be challenging. Time-lapse microscopy (140) offers an elegant solution if SAR11
763 can be maintained for the requisite time periods for accurate measurements in a microfluidic
764 device.
765 In addition to identifying taxa whose isolation success suggested deviations from
766 biological assumptions of single planktonic cells with 100% viability, the model also revealed
767 the limitations of DTE cultivation in assessing viability depending on relative abundance (Fig.
768 S9). We cannot ascertain whether any given taxon may violate an assumption of $V = 100\%$
769 unless we have enough wells to demonstrate that it grew in fewer wells than expected. For
770 example, taxa at 1% of the microbial community require more than 1,000 wells before the lack
771 of a cultured organism represents a significant negative event, rather than a taxon simply lacking
772 sufficient abundance to ensure inclusion in a well within 95% CI. In our 460 well experiments,
773 we could not resolve whether taxa may have had viabilities below 100% if they were less than
774 3% of the community for any given experiment (Fig. S9). Modeling DTE experiments showed
775 that for experiments targeting rare taxa, lower inoculum sizes are favoured where selective media
776 for enrichment is either unknown or undesirable. The exponential increase in the number of
777 required wells with respect to the inoculum size is a function of a pure well requiring *all* cells
778 within it to belong to the same taxon, assuming all cells are equally and optimally viable.
779 By providing taxon-specific predictions of viability from cultivation data, our model now
780 facilitates an iterative process to improve experimental design and make cultivation more
781 reliable. First, we use the cultivation success rates to determine for which taxa the assumption of
782 100% viability was violated. Second, we use the model to estimate viability for those organisms.
783 Third, we use the viability and relative abundance data to determine, within 95% CI, the
784 appropriate number of inoculation attempts required to isolate a new version of that organism.
785 Using SAR11 LD12 as an example, given a relative abundance of 10%, and a viability of 15%,
786 800 DTE wells should yield four pure, positive wells (1-8 95% CI). This means that, for
787 microorganisms that we know successfully grow in our media, we can now statistically constrain
788 the appropriate number of wells required to culture a given taxon again. For organisms that were
789 not abundant enough to estimate viability using the model, we can use a conservative viability
790 assumption (e.g., 50% (111)) with which to base our cultivation strategy, thereby still reducing
791 uncertainty about the experimental effort necessary to re-isolate one of these microorganisms.

Conclusions

This work has provided hundreds of new cultures for microbiological research, many among the most abundant members of the nGOM coastal bacterioplankton community. It also provides another demonstration of the effectiveness of sustained cultivation efforts for bringing previously uncultivated strains into culture. Our modeled cultivation results have generated compelling evidence for low viability within subpopulations of SAR11 LD12 and IIIa.1, as well as OM43 *Betaproteobacteria*. The prevalence of, and controls on, dormancy in these clades deserves further study. We anticipate that future work with larger DTE experiments will yield similar viability data about other groups of taxa with lower abundance, highlighting a valuable diagnostic application of DTE cultivation/modeling beyond the primary role in isolating new microorganisms. The integration of cultivation results, natural abundance data from inoculum communities, and DTE modeling represents an important step forward in quantifying the risk associated with DTE efforts to isolate valuable taxa from new sources, or repeating isolation from the same locations. We hope variations of this approach will be incorporated into wider community efforts to invest in culturing the uncultured.

Acknowledgments

We would like to thank Dr. Nancy Rabalais for her comments and edits on a very early draft of this manuscript. Portions of this research were conducted with high-performance computing resources provided by Louisiana State University (http://www.hpc.lsu.edu) and the University of Southern California (http://hpc.usc.edu).

Funding Information

This work was supported by the Department of Biological Sciences at Louisiana State University, a Louisiana Board of Regents grant to JCT (LEQSF(2014-17)-RD-A-06), a National Academies of Science, Engineering, and Medicine Gulf Research Program Early Career Fellowship to JCT, and the Dornsife College of Letters, Arts and Sciences at the University of Southern California. BT was partially funded by NERC award NE/R010935/1 and by the Simons Foundation BIOS-SCOPE program. The funders had no role in study design, data collection, and interpretation, or the decision to submit the work for publication.

Author Contributions

MWH led sample collections, cultivation experiments, nucleic acid extraction, amplicon sequencing, and analyses; VCL, DMP, JLW, and AML supported sample collections, cultivation experiments, and nucleic acid extractions; MWH and JCT conducted cultivation comparisons and phylogenetic analyses; BT developed the viability model and led the statistical analyses; CC derived the cell-specific growth rate equations incorporating viability; JCT designed the study and assisted with sample collections and model refinement; MWH, BT, and JCT led manuscript writing; and all authors contributed to and reviewed the text.

Figures

Figure 1. Percent identity of LSUCC isolate 16S rRNA genes compared with those from other isolates in NCBI ("Other", gray dots) or from the DTE culture collections IMCC (gold dots), HTCC (blue dots), and HIMB (green dots). Each dot represents a pairwise 16S rRNA gene comparison (via BLASTn). X-axis categories are groups designated according to ≥ 94% sequence identity and phylogenetic placement (see Figs S1-S4). Above the graph is the 16S rRNA gene sequence percent identity to the closest non-LSUCC isolate within a column. Groups colored in red indicate those where LSUCC isolates represent putatively novel genera, whereas orange indicates putatively novel species.

Figure 2. A global map of the isolation location of isolates from selected important aquatic bacterioplankton clades. All depicted taxa were isolated from surface water (< 1-20m), or the depth of sample was not reported (see Table S1 for details). Circles represent LSUCC isolates, while triangles are non-LSUCC isolates. Inset: a zoomed view of the coastal Louisiana region where LSUCC bacterioplankton originated.

Figure 3. Rank abundances of the 50 most abundant OTUs from all sites based on median relative abundance at salinities less than seven (A) and greater than twelve (B). The boxes indicate the interquartile range (IQR) of the data, with vertical lines indicating the upper and lower extremes according to 1.5 x IQR. Horizontal lines within each box indicate the median. The data points comprising the distribution are plotted on top of the boxplots. The shade of the dot represents the salinity at the sample site (red-blue :: lower-higher), while the color of the box indicates broad taxonomic identity. LSUCC labels indicate OTUs with at least one cultivated representative.

Figure 4. Rank abundances of the 50 most abundant ASVs from all sites based on median relative abundance at salinities less than seven (A) and greater than twelve (B). The boxes indicate the interquartile range (IQR) of the data, with vertical lines indicating the upper and lower extremes according to 1.5 x IQR. Horizontal lines within each box indicate the median. The data points comprising the distribution are plotted on top of the boxplots. The shade of the dot represents the salinity at the sample site (red-blue :: lower-higher), while the color of the box indicates broad taxonomic identity. LSUCC labels indicate ASVs with at least one cultivated representative.

Figure 5. Relative abundance of ASVs within key taxonomic groups compared with salinity. ASV types are colored independently, and triangle points indicate experiments for which at least one isolate was obtained. Non-linear regression lines are provided as a visual aid for abundance trends.

Figure 6. Graphical depiction of the viability model.

Figure 7. Actual vs. expected numbers of isolates. Each point represents the actual number of isolates for every ASV/experiment pair compared to the expected number of isolates based on our model assuming 100% viability. Colors represent the relationship to the model predictions: green- isolates within the 95% CI for expected frequency, orange- actual isolates > maximum

884 95% CI for expected isolates; blue- actual isolates < minimum 95% CI for expected isolates.
885 Circle size is proportional to the deviation of the number of actual isolates from the maximum
886 (for orange) or minimum (for blue) 95% CI for expected isolates. The dotted line is the 1:1 ratio.
887 Notable taxa on the extremities of the actual and expected values are labeled. All datapoints
888 provided in Table S1.
889
890

References

1. Metcalf WW, Griffin BM, Cicchillo RM, Gao J, Janga SC, Cooke HA, Circello BT, Evans BS, Martens-Habbena W, Stahl DA, van der Donk WA. 2012. Synthesis of methylphosphonic acid by marine microbes: a source for methane in the aerobic ocean. Science 337:1104–1107.

2. Carini P, White AE, Campbell EO, Giovannoni SJ. 2014. Methane production by phosphate-starved SAR11 chemoheterotrophic marine bacteria. Nat Commun 5:4346.

3. Karl DM, Beversdorf L, Björkman KM, Church MJ, Martinez A, Delong EF. 2008. Aerobic production of methane in the sea. Nat Geosci 1:473–478.

4. Steindler L, Schwalbach MS, Smith DP, Chan F, Giovannoni SJ. 2011. Energy starved Candidatus Pelagibacter ubique substitutes light-mediated ATP production for endogenous carbon respiration. PLoS One 6:e19725.

5. Gómez-Consarnau L, González JM, Coll-Lladó M, Gourdon P, Pascher T, Neutze R, Pedrós-Alió C, Pinhassi J. 2007. Light stimulates growth of proteorhodopsin-containing marine Flavobacteria. Nature 445:210–213.

6. Daims H, Lebedeva EV, Pjevac P, Han P, Herbold C, Albertsen M, Jehmlich N, Palatinszky M, Vierheilig J, Bulaev A, Kirkegaard RH, von Bergen M, Rattei T, Bendinger B, Nielsen PH, Wagner M. 2015. Complete nitrification by Nitrospira bacteria. Nature 528:504–509.

7. Lam KS. 2006. Discovery of novel metabolites from marine actinomycetes. Curr Opin Microbiol 9:245–251.

8. Jensen PR, Williams PG, Oh D-C, Zeigler L, Fenical W. 2007. Species-specific secondary metabolite production in marine actinomycetes of the genus Salinispora. Appl Environ Microbiol 73:1146–1152.

9. Nett M, Erol Ö, Kehraus S, Köck M, Krick A, Eguereva E, Neu E, König GM. 2006. Siphonazole, an Unusual Metabolite from Herpetosiphon sp. Angew Chem Int Ed 45:3863–3867.

10. Ling LL, Schneider T, Peoples AJ, Spoering AL, Engels I, Conlon BP, Mueller A, Schäberle TF, Hughes DE, Epstein S, Jones M, Lazarides L, Steadman VA, Cohen DR, Felix CR, Fetterman KA, Millett WP, Nitti AG, Zullo AM, Chen C, Lewis K. 2015. A new antibiotic kills pathogens without detectable resistance. Nature 517:455–459.

11. Lloyd KG, Steen AD, Ladau J, Yin J, Crosby L. 2018. Phylogenetically Novel Uncultured Microbial Cells Dominate Earth Microbiomes. mSystems 3:e00055–18.

12. Hug LA. 2018. Sizing Up the Uncultured Microbial Majority. mSystems 3:e00185–18.

13. Steen AD, Crits-Christoph A, Carini P, DeAngelis KM, Fierer N, Lloyd KG, Thrash JC. 2019. High proportions of bacteria and archaea across most biomes remain uncultured.

926 ISME J 13:3126–3130.

927 14. Overmann J, Abt B, Sikorski J. 2017. Present and Future of Culturing Bacteria. Annu Rev
928 Microbiol 71:711–730.

929 15. Rappé MS. 2013. Stabilizing the foundation of the house that 'omics builds: the evolving
930 value of cultured isolates to marine microbiology. Curr Opin Microbiol 16:618–624.

931 16. Carini P. 2019. A "Cultural" Renaissance: Genomics Breathes New Life into an Old Craft.
932 mSystems 4:e00092–19.

933 17. Staley JT, Konopka A. 1985. Measurement of in situ activities of nonphotosynthetic
934 microorganisms in aquatic and terrestrial habitats. Annu Rev Microbiol 39:321–346.

935 18. Amann RI, Ludwig W, Schleifer KH. 1995. Phylogenetic identification and in situ detection
936 of individual microbial cells without cultivation. Microbiol Rev 59:143–169.

937 19. Hahn MW, Koll U, Schmidt J. 2019. Isolation and Cultivation of Bacteria, p. 313–351. *In*
938 Hurst, CJ (ed.), The Structure and Function of Aquatic Microbial Communities. Springer
939 International Publishing, Cham.

940 20. Kaeberlein T, Lewis K, Epstein SS. 2002. Isolating "uncultivable" microorganisms in pure
941 culture in a simulated natural environment. Science 296:1127–1129.

942 21. Zengler K, Toledo G, Rappe M, Elkins J, Mathur EJ, Short JM, Keller M. 2002. Cultivating
943 the uncultured. Proc Natl Acad Sci U S A 99:15681–15686.

944 22. Steinert G, Whitfield S, Taylor MW, Thoms C, Schupp PJ. 2014. Application of Diffusion
945 Growth Chambers for the Cultivation of Marine Sponge-Associated Bacteria. Mar
946 Biotechnol 16:594–603.

947 23. Nichols D, Cahoon N, Trakhtenberg EM, Pham L, Mehta A, Belanger A, Kanigan T, Lewis
948 K, Epstein SS. 2010. Use of Ichip for High-Throughput In Situ Cultivation of
949 "Uncultivable" Microbial Species. Appl Environ Microbiol 76:2445–2450.

950 24. Tandogan N, Abadian PN, Epstein S, Aoi Y, Goluch ED. 2014. Isolation of microorganisms
951 using sub-micrometer constrictions. PLoS One 9:e101429.

952 25. Hahn MW, Stadler P, Wu QL, Pöckl M. 2004. The filtration–acclimatization method for
953 isolation of an important fraction of the not readily cultivable bacteria. J Microbiol Methods
954 57:379–390.

955 26. Connon SA, Giovannoni SJ. 2002. High-throughput methods for culturing microorganisms
956 in very-low-nutrient media yield diverse new marine isolates. Appl Environ Microbiol
957 68:3878–3885.

958 27. Yang SJ, Kang I, Cho JC. 2016. Expansion of Cultured Bacterial Diversity by Large-Scale
959 Dilution-to-Extinction Culturing from a Single Seawater Sample. Microb Ecol 71:29–43.

960 28. Stingl U, Tripp HJ, Giovannoni SJ. 2007. Improvements of high-throughput culturing
961 yielded novel SAR11 strains and other abundant marine bacteria from the Oregon coast and
962 the Bermuda Atlantic Time Series study site. ISME J 1:361–371.

963 29. Henson MW, Lanclos VC, Faircloth BC, Thrash JC. 2018. Cultivation and genomics of the
964 first freshwater SAR11 (LD12) isolate. ISME J 12:1846–1860.

965 30. Hahnke RL, Bennke CM, Fuchs BM, Mann AJ, Rhiel E, Teeling H, Amann R, Harder J.
966 2015. Dilution cultivation of marine heterotrophic bacteria abundant after a spring
967 phytoplankton bloom in the North Sea. Environ Microbiol 17:3515–3526.

968 31. Sosa OA, Gifford SM, Repeta DJ, DeLong EF. 2015. High molecular weight dissolved
969 organic matter enrichment selects for methylotrophs in dilution to extinction cultures. ISME
970 J 9:2725–2739.

971 32. Schut F, de Vries EJ, Gottschal JC, Robertson BR, Harder W, Prins RA, Button DK. 1993.
972 Isolation of Typical Marine Bacteria by Dilution Culture: Growth, Maintenance, and
973 Characteristics of Isolates under Laboratory Conditions. Appl Environ Microbiol 59:2150–
974 2160.

975 33. Button DK, Schut F, Quang P, Martin R, Robertson BR. 1993. Viability and isolation of
976 marine bacteria by dilution culture: theory, procedures, and initial results. Appl Environ
977 Microbiol 59:881–891.

978 34. Song J, Oh HM, Cho JC. 2009. Improved culturability of SAR11 strains in dilution-to-
979 extinction culturing from the East Sea, West Pacific Ocean. FEMS Microbiol Lett 295:141–
980 147.

981 35. Henson MW, Pitre DM, Weckhorst JL, Lanclos VC, Webber AT, Thrash JC. 2016.
982 Artificial Seawater Media Facilitate Cultivating Members of the Microbial Majority from
983 the Gulf of Mexico. mSphere 1:e00028–16.

984 36. Rappé MS, Connon SA, Vergin KL, Giovannoni SJ. 2002. Cultivation of the ubiquitous
985 SAR11 marine bacterioplankton clade. Nature 418:630–633.

986 37. Marshall KT, Morris RM. 2013. Isolation of an aerobic sulfur oxidizer from the
987 SUP05/Arctic96BD-19 clade. ISME J 7:452–455.

988 38. Shah V, Chang BX, Morris RM. 2017. Cultivation of a chemoautotroph from the SUP05
989 clade of marine bacteria that produces nitrite and consumes ammonium. ISME J 11:263–
990 271.

991 39. Spietz RL, Lundeen RA, Zhao X, Nicastro D, Ingalls AE, Morris RM. 2019. Heterotrophic
992 carbon metabolism and energy acquisition in Candidatus Thioglobus singularis strain PS1, a
993 member of the SUP05 clade of marine Gammaproteobacteria. Environ Microbiol 21:2391–
994 2401.

995 40. Huggett MJ, Hayakawa DH, Rappé MS. 2012. Genome sequence of strain HIMB624, a

cultured representative from the OM43 clade of marine Betaproteobacteria. Stand Genomic Sci 6:11–20.

41. Giovannoni SJ, Hayakawa DH, Tripp HJ, Stingl U, Givan SA, Cho J-C, Oh H-M, Kitner JB, Vergin KL, Rappé MS. 2008. The small genome of an abundant coastal ocean methylotroph. Environ Microbiol 10:1771–1782.

42. Durham BP, Grote J, Whittaker KA, Bender SJ, Luo H, Grim SL, Brown JM, Casey JR, Dron A, Florez-Leiva L, Others. 2014. Draft genome sequence of marine alphaproteobacterial strain HIMB11, the first cultivated representative of a unique lineage within the Roseobacter clade possessing an unusually small genome. Stand Genomic Sci 9:632–645.

43. Cho JC, Giovannoni SJ. 2004. Cultivation and Growth Characteristics of a Diverse Group of Oligotrophic Marine Gammaproteobacteria. Appl Environ Microbiol 70:432–440.

44. Kim S, Kang I, Seo J-H, Cho J-C. 2019. Culturing the ubiquitous freshwater actinobacterial acI lineage by supplying a biochemical “helper”catalase. ISME J 13:2252–2263.

45. Tripp HJ. 2013. The unique metabolism of SAR11 aquatic bacteria. J Microbiol 51:147–153.

46. Nichols D, Lewis K, Orjala J, Mo S, Ortenberg R, O’Connor P, Zhao C, Vouros P, Kaeberlein T, Epstein SS. 2008. Short Peptide Induces an “Uncultivable” Microorganism To Grow In Vitro. Appl Environ Microbiol 74:4889–4897.

47. Stewart EJ. 2012. Growing unculturable bacteria. J Bacteriol 194:4151–4160.

48. Kell DB, Young M. 2000. Bacterial dormancy and culturability: the role of autocrine growth factors. Curr Opin Microbiol 3:238–243.

49. Carini P, Steindler L, Beszteri S, Giovannoni SJ. 2013. Nutrient requirements for growth of the extreme oligotroph “Candidatus Pelagibacter ubique” HTCC1062 on a defined medium. ISME J 7:592–602.

50. Epstein SS. 2013. The phenomenon of microbial uncultivability. Curr Opin Microbiol 16:636–642.

51. Shah D, Zhang Z, Khodursky A, Kaldalu N, Kurg K, Lewis K. 2006. Persisters: a distinct physiological state of E. coli. BMC Microbiol 6:53.

52. Kell D, Potgieter M, Pretorius E. 2015. Individuality, phenotypic differentiation, dormancy and “persistence” in culturable bacterial systems: commonalities shared by environmental, laboratory, and clinical microbiology. F1000Res 4:179.

53. Lennon JT, Jones SE. 2011. Microbial seed banks: the ecological and evolutionary implications of dormancy. Nat Rev Microbiol 9:119–130.

54. Grassi L, Di Luca M, Maisetta G, Rinaldi AC, Esin S, Trampuz A, Batoni G. 2017. Generation of persister cells of Pseudomonas aeruginosa and Staphylococcus aureus by chemical treatment and evaluation of their susceptibility to membrane-targeting agents. Front Microbiol 8:1917.

55. Bergkessel M, Basta DW, Newman DK. 2016. The physiology of growth arrest: uniting molecular and environmental microbiology. Nat Rev Microbiol 14:549–562.

56. Kussell E, Leibler S. 2005. Phenotypic diversity, population growth, and information in fluctuating environments. Science 309:2075–2078.

57. Kurm V, van der Putten WH, Gera Hol WH. 2019. Cultivation-success of rare soil bacteria is not influenced by incubation time and growth medium. PLoS One 14:e0210073.

58. D'Onofrio A, Crawford JM, Stewart EJ, Witt K, Gavrish E, Epstein S, Clardy J, Lewis K. 2010. Siderophores from neighboring organisms promote the growth of uncultured bacteria. Chem Biol 17:254–264.

59. Thrash JC. 2019. Culturing the Uncultured: Risk versus Reward. mSystems 4:e00130–19.

60. Thrash JC, Weckhorst JL, Pitre DM. 2017. Cultivating Fastidious Microbes, p. 57–78. *In* McGenity, TJ, Timmis, KN, Nogales, B (eds.), Hydrocarbon and Lipid Microbiology Protocols. Springer Berlin Heidelberg, Berlin, Heidelberg.

61. Vila-Costa M, Simó R, Harada H, Gasol JM, Slezak D, Kiene RP. 2006. Dimethylsulfoniopropionate uptake by marine phytoplankton. Science 314:652–654.

62. Mou X, Hodson RE, Moran MA. 2007. Bacterioplankton assemblages transforming dissolved organic compounds in coastal seawater. Environ Microbiol 9:2025–2037.

63. Stein LY. 2015. Microbiology: Cyanate fuels the nitrogen cycle. Nature 524:43–44.

64. Repeta DJ, Ferrón S, Sosa OA, Johnson CG, Repeta LD, Acker M, Delong EF, Karl DM. 2016. Marine methane paradox explained by bacterial degradation of dissolved organic matter. Nat Geosci 9:884–887.

65. Curson ARJ, Liu J, Bermejo Martínez A, Green RT, Chan Y, Carrión O, Williams BT, Zhang S-H, Yang G-P, Bulman Page PC, Zhang X-H, Todd JD. 2017. Dimethylsulfoniopropionate biosynthesis in marine bacteria and identification of the key gene in this process. Nat Microbiol 2:17009.

66. Widner B, Mulholland MR. 2017. Cyanate distribution and uptake in North Atlantic coastal waters. Limnol Oceanogr 62:2538–2549.

67. Widner B, Mulholland MR, Mopper K. 2016. Distribution, Sources, and Sinks of Cyanate in the Coastal North Atlantic Ocean. Environ Sci Technol Lett 3:297–302.

68. Henson MW, Hanssen J, Spooner G, Fleming P, Pukonen M, Stahr F, Thrash JC. 2018.

1064 Nutrient dynamics and stream order influence microbial community patterns along a 2914
1065 kilometer transect of the Mississippi River. Limnol Oceanogr 63:1837–1855.

1066 69. Apprill A, McNally S, Parsons R, Weber L. 2015. Minor revision to V4 region SSU rRNA
1067 806R gene primer greatly increases detection of SAR11 bacterioplankton. Aquat Microb
1068 Ecol 75:129–137.

1069 70. Walters W, Hyde ER, Berg-Lyons D, Ackermann G, Humphrey G, Parada A, Gilbert JA,
1070 Jansson JK, Caporaso JG, Fuhrman JA, Apprill A, Knight R. 2016. Improved Bacterial 16S
1071 rRNA Gene (V4 and V4-5) and Fungal Internal Transcribed Spacer Marker Gene Primers
1072 for Microbial Community Surveys. mSystems 1:e00009–15.

1073 71. Schloss PD, Westcott SL, Ryabin T, Hall JR, Hartmann M, Hollister EB, Lesniewski R a.,
1074 Oakley BB, Parks DH, Robinson CJ, Sahl JW, Stres B, Thallinger GG, Van Horn DJ,
1075 Weber CF. 2009. Introducing mothur: Open-source, platform-independent, community-
1076 supported software for describing and comparing microbial communities. Appl Environ
1077 Microbiol 75:7537–7541.

1078 72. Pruesse E, Quast C, Knittel K, Fuchs BM, Ludwig W, Peplies J, Glockner FO, Glöckner
1079 FO. 2007. SILVA: a comprehensive online resource for quality checked and aligned
1080 ribosomal RNA sequence data compatible with ARB. Nucleic Acids Res 35:7188–7196.

1081 73. Quast C, Pruesse E, Yilmaz P, Gerken J, Schweer T, Yarza P, Peplies J, Glöckner FO.
1082 2013. The SILVA ribosomal RNA gene database project: Improved data processing and
1083 web-based tools. Nucleic Acids Res 41:590–596.

1084 74. Eren AM, Borisy GG, Huse SM, Mark Welch JL. 2014. Oligotyping analysis of the human
1085 oral microbiome. Proc Natl Acad Sci U S A 111:E2875–84.

1086 75. Fujimoto M, Cavaletto J, Liebig JR, McCarthy A, Vanderploeg HA, Denef VJ. 2016.
1087 Spatiotemporal distribution of bacterioplankton functional groups along a freshwater
1088 estuary to pelagic gradient in Lake Michigan. J Great Lakes Res 42:1036–1048.

1089 76. Cole JR, Wang Q, Fish JA, Chai B, McGarrell DM, Sun Y, Brown CT, Porras-Alfaro A,
1090 Kuske CR, Tiedje JM. 2014. Ribosomal Database Project: data and tools for high
1091 throughput rRNA analysis. Nucleic Acids Res 42:D633–42.

1092 77. Team RC. 2017. R Core Team (2017). R: A language and environment for statistical
1093 computing. R Found Stat Comput Vienna, Austria URL http://www R-project org/ , page R
1094 Foundation for Statistical Computing.

1095 78. McMurdie PJ, Holmes S. 2013. phyloseq: An R Package for Reproducible Interactive
1096 Analysis and Graphics of Microbiome Census Data. PLoS One 8:e61217.

1097 79. Camacho C, Coulouris G, Avagyan V, Ma N, Papadopoulos J, Bealer K, Madden TL. 2009.
1098 BLAST+: architecture and applications. BMC Bioinformatics 10:421.

1099 80. Edgar RC. 2004. MUSCLE: multiple sequence alignment with high accuracy and high

throughput. Nucleic Acids Res 32:1792–1797.

81. Capella-Gutiérrez S, Silla-Martínez JM, Gabaldón T. 2009. trimAl: a tool for automated alignment trimming in large-scale phylogenetic analyses. Bioinformatics 25:1972–1973.

82. Nguyen L-T, Schmidt HA, von Haeseler A, Minh BQ. 2015. IQ-TREE: a fast and effective stochastic algorithm for estimating maximum-likelihood phylogenies. Mol Biol Evol 32:268–274.

83. Hoang DT, Chernomor O, von Haeseler A, Minh BQ, Vinh LS. 2018. UFBoot2: Improving the Ultrafast Bootstrap Approximation. Mol Biol Evol 35:518–522.

84. Junier T, Zdobnov EM. 2010. The Newick utilities: high-throughput phylogenetic tree processing in the UNIX shell. Bioinformatics 26:1669–1670.

85. Han MV, Zmasek CM. 2009. phyloXML: XML for evolutionary biology and comparative genomics. BMC Bioinformatics 10:356.

86. Stingl U, Cho JC, Foo W, Vergin KL, Lanoil B, Giovannoni SJ. 2008. Dilution-to-extinction culturing of psychrotolerant planktonic bacteria from permanently ice-covered lakes in the McMurdo Dry Valleys, Antarctica. Microb Ecol 55:395–405.

87. Page KA, Connon SA, Giovannoni SJ. 2004. Representative freshwater bacterioplankton isolated from Crater Lake, Oregon. Appl Environ Microbiol 70:6542–6550.

88. Noell SE, Giovannoni SJ. 2019. SAR11 bacteria have a high affinity and multifunctional glycine betaine transporter. Environ Microbiol 21:2559–2575.

89. Thume K, Gebser B, Chen L, Meyer N, Kieber DJ, Pohnert G. 2018. The metabolite dimethylsulfoxonium propionate extends the marine organosulfur cycle. Nature 563:412–415.

90. Asher EC, Dacey JWH, Stukel M, Long MC, Tortell PD. 2017. Processes driving seasonal variability in DMS, DMSP, and DMSO concentrations and turnover in coastal Antarctic waters. Limnol Oceanogr 62:104–124.

91. Mizuno CM, Rodriguez-Valera F, Ghai R. 2015. Genomes of planktonic Acidimicrobiales: widening horizons for marine Actinobacteria by metagenomics. MBio 6:e02083–14.

92. Lee J, Kwon KK, Lim S-I, Song J, Choi AR, Yang S-H, Jung K-H, Lee J-H, Kang SG, Oh H-M, Cho JC. 2019. Isolation, cultivation, and genome analysis of proteorhodopsin-containing SAR116-clade strain Candidatus Puniceispirillum marinum IMCC1322. J Microbiol 57:676–687.

93. Kitzinger K, Padilla CC, Marchant HK, Hach PF, Herbold CW, Kidane AT, Könneke M, Littmann S, Mooshammer M, Niggemann J, Petrov S, Richter A, Stewart FJ, Wagner M, Kuypers MMM, Bristow LA. 2019. Cyanate and urea are substrates for nitrification by Thaumarchaeota in the marine environment. Nat Microbiol 4:234–243.

1135 94. Kamennaya NA, Post AF. 2011. Characterization of cyanate metabolism in marine
1136 Synechococcus and Prochlorococcus spp. Appl Environ Microbiol 77:291–301.

1137 95. Eren AM, Maignien L, Sul WJ, Murphy LG, Grim SL, Morrison HG, Sogin ML. 2013.
1138 Oligotyping: Differentiating between closely related microbial taxa using 16S rRNA gene
1139 data. Methods Ecol Evol 4:1111–1119.

1140 96. Needham DM, Fuhrman JA. 2016. Pronounced daily succession of phytoplankton, archaea
1141 and bacteria following a spring bloom. Nat Microbiol 1:16005.

1142 97. Campbell BJ, Yu L, Heidelberg JF, Kirchman DL. 2011. Activity of abundant and rare
1143 bacteria in a coastal ocean. Proc Natl Acad Sci U S A 108:12776–12781.

1144 98. Oh HM, Kwon KK, Kang I, Kang SG, Lee JH, Kim SJ, Cho JC. 2010. Complete genome
1145 sequence of "Candidatus puniceispirillum marinum" IMCC1322, a representative of the
1146 SAR116 clade in the Alphaproteobacteria. J Bacteriol 192:3240–3241.

1147 99. Fegatella F, Lim J, Kjelleberg S, Cavicchioli R. 1998. Implications of rRNA operon copy
1148 number and ribosome content in the marine oligotrophic ultramicrobacterium
1149 Sphingomonas sp. strain RB2256. Appl Environ Microbiol 64:4433–4438.

1150 100. Acinas SG, Marcelino LA, Klepac-Ceraj V, Polz MF. 2004. Divergence and redundancy
1151 of 16S rRNA sequences in genomes with multiple rrn operons. J Bacteriol 186:2629–2635.

1152 101. Pedrós-Alió C. 2012. The rare bacterial biosphere. Ann Rev Mar Sci 4:449–466.

1153 102. Martiny AC. 2019. High proportions of bacteria are culturable across major biomes.
1154 ISME J 13:2125–2128.

1155 103. Parada AE, Needham DM, Fuhrman JA. 2015. Every base matters: assessing small
1156 subunit rRNA primers for marine microbiomes with mock communities, time series and
1157 global field samples. Environ Microbiol 18:1403–1414.

1158 104. Del Giorgio PA, Gasol JM. 2008. Physiological structure and single-cell activity in
1159 marine bacterioplankton. Microbial Ecology of the Oceans 2:243–298.

1160 105. Malmstrom RR, Kiene RP, Cottrell MT, Kirchman DL. 2004. Contribution of SAR11
1161 bacteria to dissolved dimethylsulfoniopropionate and amino acid uptake in the North
1162 Atlantic Ocean. Appl Environ Microbiol 70:4129–4135.

1163 106. Malmstrom RR, Cottrell MT, Elifantz H, Kirchman DL. 2005. Biomass production and
1164 assimilation of dissolved organic matter by SAR11 bacteria in the Northwest Atlantic
1165 Ocean. Appl Environ Microbiol 71:2979–2986.

1166 107. Piwosz K, Salcher MM, Zeder M, Ameryk A, Pernthaler J. 2013. Seasonal dynamics and
1167 activity of typical freshwater bacteria in brackish waters of the Gulf of Gdańsk. Limnol
1168 Oceanogr 58:817–826.

1169 108. Laghdass M, Catala P, Caparros J, Oriol L, Lebaron P, Obernosterer I. 2012. High
1170 contribution of SAR11 to microbial activity in the north west Mediterranean Sea. Microb
1171 Ecol 63:324–333.

1172 109. Salter I, Galand PE, Fagervold SK, Lebaron P, Obernosterer I, Oliver MJ, Suzuki MT,
1173 Tricoire C. 2015. Seasonal dynamics of active SAR11 ecotypes in the oligotrophic
1174 Northwest Mediterranean Sea. ISME J 9:347–360.

1175 110. Leizeaga A, Estrany M, Forn I, Sebastián M. 2017. Using Click-Chemistry for
1176 Visualizing in Situ Changes of Translational Activity in Planktonic Marine Bacteria. Front
1177 Microbiol 8:2360.

1178 111. Kirchman DL. 2016. Growth Rates of Microbes in the Oceans. Ann Rev Mar Sci 8:285–
1179 309.

1180 112. Samo TJ, Smriga S, Malfatti F, Sherwood BP, Azam F. 2014. Broad distribution and high
1181 proportion of protein synthesis active marine bacteria revealed by click chemistry at the
1182 single cell level. Frontiers in Marine Science 1:48.

1183 113. Smriga S, Samo TJ, Malfatti F, Villareal J, Azam F. 2014. Individual cell DNA synthesis
1184 within natural marine bacterial assemblages as detected by “click”chemistry. Aquat Microb
1185 Ecol 72:269–280.

1186 114. Bradley JA, Amend JP, LaRowe DE. 2019. Survival of the fewest: Microbial dormancy
1187 and maintenance in marine sediments through deep time. Geobiology 17:43–59.

1188 115. Zhao Y, Temperton B, Thrash JC, Schwalbach MS, Vergin KL, Landry ZC, Ellisman M,
1189 Deerinck T, Sullivan MB, Giovannoni SJ. 2013. Abundant SAR11 viruses in the ocean.
1190 Nature 494:357–360.

1191 116. Martinez-Hernandez F, Fornas Ò, Lluesma Gomez M, Garcia-Heredia I, Maestre-
1192 Carballa L, López-Pérez M, Haro-Moreno JM, Rodriguez-Valera F, Martinez-Garcia M.
1193 2018. Single-cell genomics uncover Pelagibacter as the putative host of the extremely
1194 abundant uncultured 37-F6 viral population in the ocean. ISME J 13:232–236.

1195 117. Chen L-X, Zhao Y, McMahon KD, Mori JF, Jessen GL, Nelson TC, Warren LA,
1196 Banfield JF. 2019. Wide Distribution of Phage That Infect Freshwater SAR11 Bacteria.
1197 mSystems 4:e00410–19.

1198 118. Thingstad TF, Lignell R. 1997. Theoretical models for the control of bacterial growth
1199 rate, abundance, diversity and carbon demand. Aquat Microb Ecol 13:19–27.

1200 119. Våge S, Storesund JE, Thingstad TF. 2013. SAR11 viruses and defensive host strains.
1201 Nature 499:E3–4.

1202 120. Thingstad TF, Vage S, Storesund JE, Sandaa RA, Giske J. 2014. A theoretical analysis of
1203 how strain-specific viruses can control microbial species diversity. Proc Natl Acad Sci U S
1204 A 111:7813–7818.

121. Giovannoni S, Temperton B, Zhao Y. 2013. Giovannoni et al. reply. Nature 499:E4–E5.

122. Alonso-Sáez L, Morán XAG, Clokie MR. 2018. Low activity of lytic pelagiphages in coastal marine waters. ISME J 12:2100–2102.

123. Chapman-McQuiston E, Wu XL. 2008. Stochastic receptor expression allows sensitive bacteria to evade phage attack. Part I: experiments. Biophys J 94:4525–4536.

124. Bertozzi Silva J, Storms Z, Sauvageau D. 2016. Host receptors for bacteriophage adsorption. FEMS Microbiol Lett 363:fnw002.

125. Williamson SJ, Houchin LA, McDaniel L, Paul JH. 2002. Seasonal variation in lysogeny as depicted by prophage induction in Tampa Bay, Florida. Appl Environ Microbiol 68:4307–4314.

126. Stough JMA, Tang X, Krausfeldt LE, Steffen MM, Gao G, Boyer GL, Wilhelm SW. 2017. Molecular prediction of lytic vs lysogenic states for Microcystis phage: Metatranscriptomic evidence of lysogeny during large bloom events. PLoS One 12:e0184146.

127. Zhao Y, Qin F, Zhang R, Giovannoni SJ, Zhang Z, Sun J, Du S, Rensing C. 2019. Pelagiphages in the Podoviridae family integrate into host genomes. Environ Microbiol 21:1989–2001.

128. Morris RM, Cain KR, Hvorecny KL, Kollman JM. 2020. Lysogenic host–virus interactions in SAR11 marine bacteria. Nature Microbiology 1–5.

129. Warwick-Dugdale J, Buchholz HH, Allen MJ, Temperton B. 2019. Host-hijacking and planktonic piracy: how phages command the microbial high seas. Virol J 16:15.

130. Yu Z-C, Chen X-L, Shen Q-T, Zhao D-L, Tang B-L, Su H-N, Wu Z-Y, Qin Q-L, Xie B-B, Zhang X-Y, Yu Y, Zhou B-C, Chen B, Zhang Y-Z. 2015. Filamentous phages prevalent in Pseudoalteromonas spp. confer properties advantageous to host survival in Arctic sea ice. ISME J 9:871–881.

131. Shkoporov AN, Khokhlova EV, Fitzgerald CB, Stockdale SR, Draper LA, Ross RP, Hill C. 2018. ΦCrAss001 represents the most abundant bacteriophage family in the human gut and infects Bacteroides intestinalis. Nat Commun 9:4781.

132. Teira E, Martínez-García S, Lønborg C, Alvarez-Salgado XA. 2009. Growth rates of different phylogenetic bacterioplankton groups in a coastal upwelling system. Environ Microbiol Rep 1:545–554.

133. Lankiewicz TS, Cottrell MT, Kirchman DL. 2016. Growth rates and rRNA content of four marine bacteria in pure cultures and in the Delaware estuary. ISME J 10:823–832.

134. Ferrera I, Gasol JM, Sebastián M, Hojerová E, Koblízek M. 2011. Comparison of growth rates of aerobic anoxygenic phototrophic bacteria and other bacterioplankton groups in

coastal Mediterranean waters. Appl Environ Microbiol 77:7451–7458.

135. Carini P, Campbell EO, Morré J, Sañudo-Wilhelmy SA, Thrash JC, Bennett SE, Temperton B, Begley T, Giovannoni SJ. 2014. Discovery of a SAR11 growth requirement for thiamin's pyrimidine precursor and its distribution in the Sargasso Sea. ISME J 8:1727–1738.

136. Grant SR, Church MJ, Ferrón S, Laws EA, Rappé MS. 2019. Elemental Composition, Phosphorous Uptake, and Characteristics of Growth of a SAR11 Strain in Batch and Continuous Culture. mSystems 4:e00218–18.

137. Simon M, Azam F. 1989. Protein content and protein synthesis rates of planktonic marine bacteria. Marine ecology progress series Oldendorf 51:201–213.

138. White AE, Giovannoni SJ, Zhao Y, Vergin K, Carlson CA. 2019. Elemental content and stoichiometry of SAR11 chemoheterotrophic marine bacteria. Limnology and Oceanography Letters 4:44–51.

139. Smith DP, Cameron Thrash J, Nicora CD, Lipton MS, Burnum-Johnson KE, Carini P, Smith RD, Giovannoni SJ. 2013. Proteomic and Transcriptomic Analyses of "Candidatus Pelagibacter ubique" Describe the First PII-Independent Response to Nitrogen Limitation in a Free-Living Alphaproteobacterium. MBio 4:e00133–12.

140. van Vliet S, Dal Co A, Winkler AR, Spriewald S, Stecher B, Ackermann M. 2018. Spatially Correlated Gene Expression in Bacterial Groups: The Role of Lineage History, Spatial Gradients, and Cell-Cell Interactions. Cell Syst 6:496–507.e6.

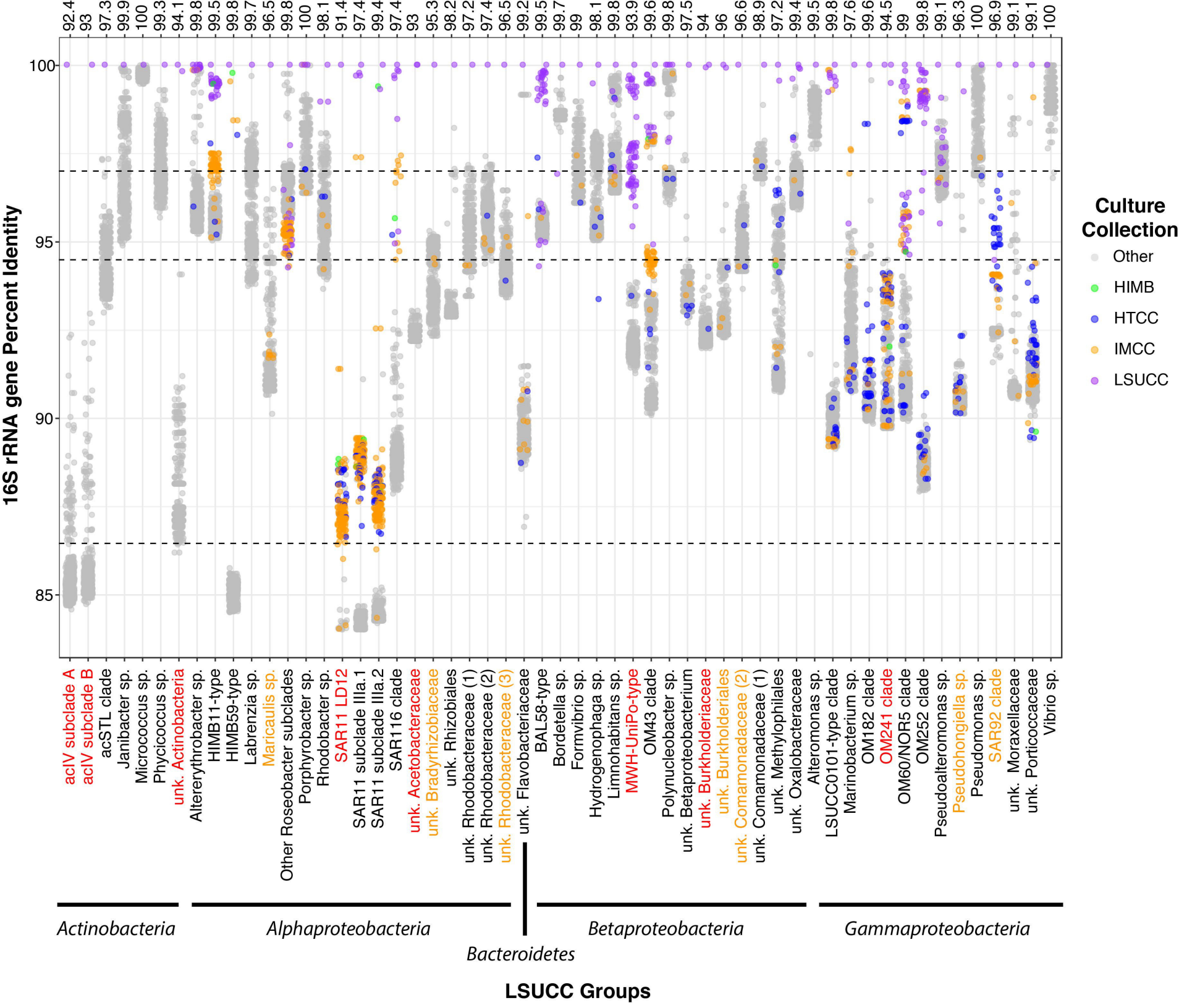
16S rRNA gene Percent Identity
100
95
90
85
Culture Collection
Other
HIMB
HTCC
IMCC
LSUCC
aclV subclade A
aclV subclade B
acSTL clade
Janibacter sp.
Micrococcus sp.
Phycicoccus sp.
unk. Actinobacteria
Altererythrobacter sp.
HIMB11-type
HIMB59-type
Labrenzia sp.
Maricaulis sp.
Other Roseobacter subclades
Porphyrobacter sp.
Rhodobacter sp.
SAR11 LD12
SAR11 subclade IIIa.1
SAR11 subclade IIIa.2
SAR116 clade
unk. Acetobacteraceae
unk. Bradyrhizobiaceae
unk. Rhizobiales
unk. Rhodobacteraceae (1)
unk. Rhodobacteraceae (2)
unk. Rhodobacteraceae (3)
unk. Flavobacteriaceae
BAL58-type
Bordetella sp.
Formvibrio sp.
Hydrogenophaga sp.
Limnohabitans sp.
MWH-UniPo-type
OM43 clade
Polynucleobacter sp.
unk. Betaproteobacterium
unk. Burkholderiaceae
unk. Burkholderiales
unk. Comamonadaceae (2)
unk. Comamonadaceae (1)
unk. Methylophilales
unk. Oxalobacteraceae
Alteromonas sp.
LSUCC0101-type clade
Marinobacterium sp.
OM182 clade
OM241 clade
OM60/NOR5 clade
OM252 clade
Pseudoalteromonas sp.
Pseudohongiella sp.
Pseudomonas sp.
SAR92 clade
unk. Moraxellaceae
unk. Porticoccaceae
Vibrio sp.
Actinobacteria
Alphaproteobacteria
Bacteroidetes
Betaproteobacteria
Gammaproteobacteria
LSUCC Groups

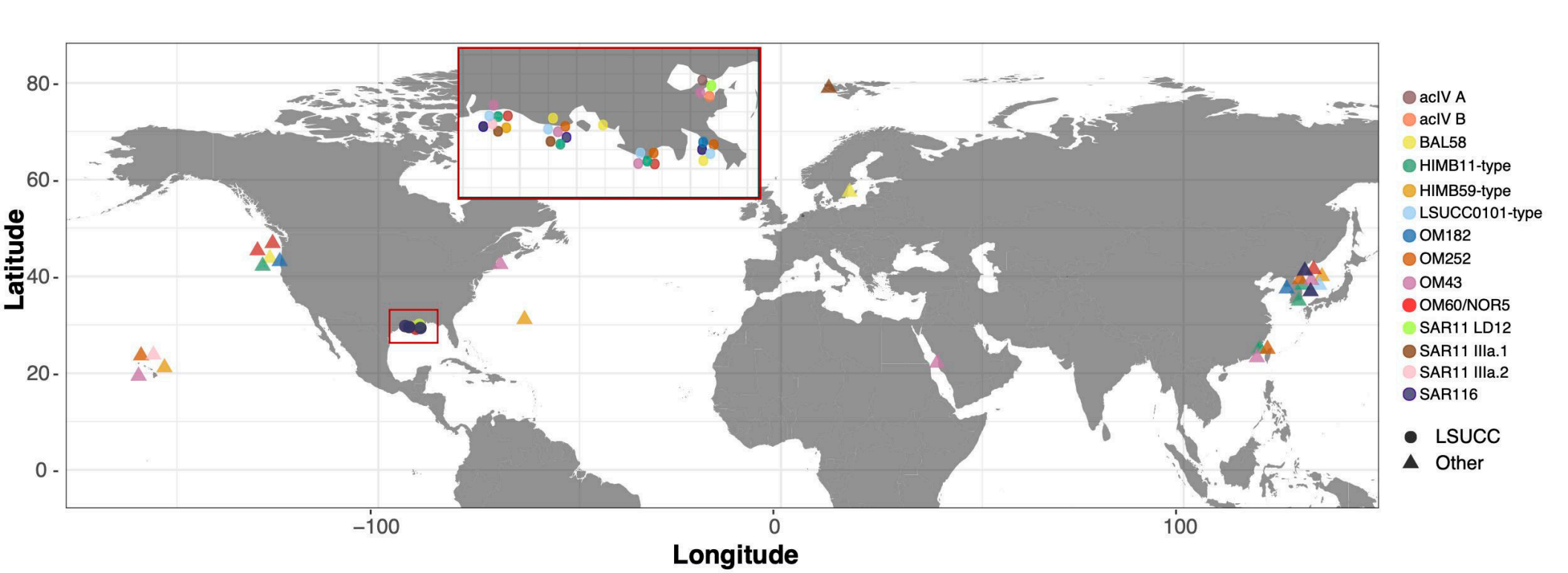
80
60
40
20
0
Latitude
−100
0
100
Longitude
acIV A
acIV B
BAL58
HIMB11-type
HIMB59-type
LSUCC0101-type
OM182
OM252
OM43
OM60/NOR5
SAR11 LD12
SAR11 IIIa.1
SAR11 IIIa.2
SAR116
LSUCC
Other

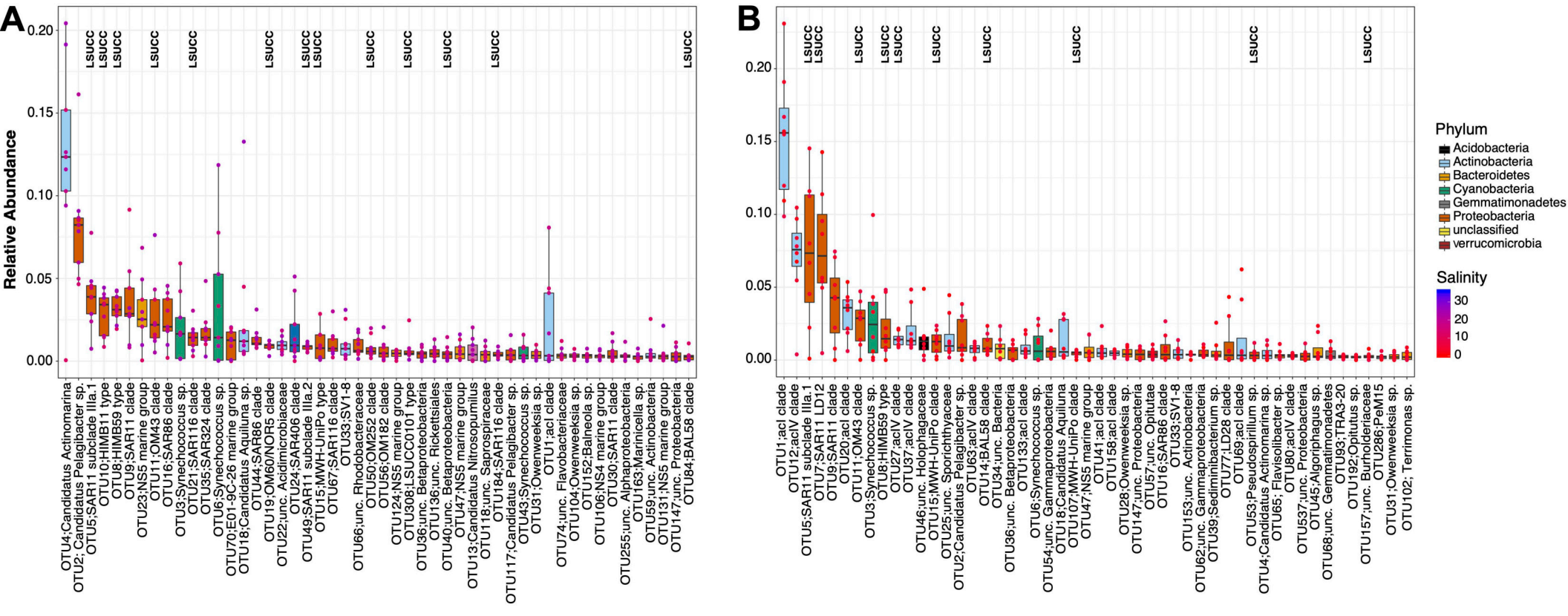
A
B
Relative Abundance
0.20
0.15
0.10
0.05
0.00
LSUCC
OTU4;Candidatus Actinomarina
OTU2; Candidatus Pelagibacter sp.
OTU5;SAR11 subclade IIIa.1
OTU10;HIMB11 type
OTU8;HIMB59 type
OTU9;SAR11 clade
OTU23;NS5 marine group
OTU11;OM43 clade
OTU16;SAR86 clade
OTU3;Synechococcus sp.
OTU21;SAR116 clade
OTU35;SAR324 clade
OTU6;Synechococcus sp.
OTU70;E01-9C-26 marine group
OTU18;Candidatus Aquiluna sp.
OTU44;SAR86 clade
OTU19;OM60/NOR5 clade
OTU22;unc. Acidimicrobiaceae
OTU24;SAR406 clade
OTU49;SAR11 subclade IIIa.2
OTU15;MWH-UniPo type
OTU67;SAR116 clade
OTU33;SV1-8
OTU66;unc. Rhodobacteraceae
OTU50;OM252 clade
OTU56;OM182 clade
OTU124;NS5 marine group
OTU308;LSUCC0101 type
OTU36;unc. Betaproteobacteria
OTU136;unc. Rickettsiales
OTU40;unc. Betaproteobacteria
OTU47;NS5 marine group
OTU13;Candidatus Nitrosopumilus
OTU118;unc. Saprospiraceae
OTU184;SAR116 clade
OTU117;Candidatus Pelagibacter sp.
OTU43;Synechococcus sp.
OTU31;Owenweeksia sp.
OTU1;acl clade
OTU74;unc. Flavobacteriaceae
OTU104;Owenweeksia sp.
OTU152;Balneola sp.
OTU106;NS4 marine group
OTU30;SAR11 clade
OTU255;unc. Alphaproteobacteria
OTU163;Marinicella sp.
OTU59;unc. Actinobacteria
OTU131;NS5 marine group
OTU147;unc. Proteobacteria
OTU84;BAL58 clade
OTU12;acl clade
OTU7;SAR11 LD12
OTU20;acl clade
OTU37;acl clade
OTU46;unc. Holophagaceae
OTU25;unc. Sporichthyaceae
OTU63;acl clade
OTU14;BAL58 clade
OTU34;unc. Bacteria
OTU133;acl clade
OTU54;unc. Gammaproteobacteria
OTU18;Candidatus Aquiluna
OTU107;MWH-UniPo clade
OTU41;acl clade
OTU158;acl clade
OTU28;Owenweeksia sp.
OTU57;unc. Opitutae
OTU153;unc. Actinobacteria
OTU62;unc. Gammaproteobacteria
OTU39;Sediminibacterium sp.
OTU77;LD28 clade
OTU53;Pseudospirillum sp.
OTU65; Flavisolibacter sp.
OTU537;unc. Proteobacteria
OTU45;Algoriphagus sp.
OTU93;TRA3-20
OTU192;Opitutus sp.
OTU286;PeM15
OTU102; Terrimonas sp.
Phylum
Acidobacteria
Actinobacteria
Bacteroidetes
Cyanobacteria
Gemmatimonadetes
Proteobacteria
unclassified
verrucomicrobia
Salinity
30
20
10
0

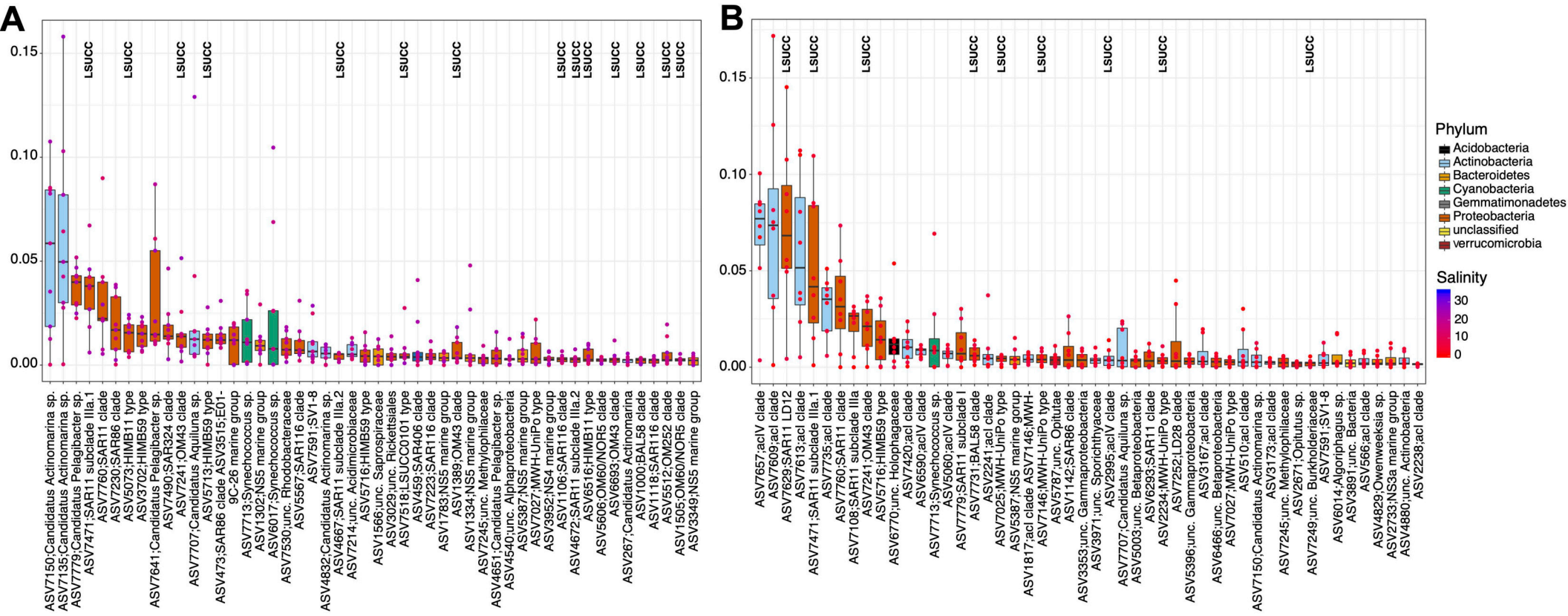
A
B
0.15
0.10
0.05
0.00
LSUCC
ASV7150;Candidatus Actinomarina sp.
ASV7135;Candidatus Actinomarina sp.
ASV7779;Candidatus Pelagibacter sp.
ASV7471;SAR11 subclade IIIa.1
ASV7760;SAR11 clade
ASV7230;SAR86 clade
ASV5073;HIMB11 type
ASV3702;HIMB59 type
ASV7641;Candidatus Pelagibacter sp.
ASV7490;SAR324 clade
ASV7241;OM43 clade
ASV7707;Candidatus Aquiluna sp.
ASV5713;HIMB59 type
ASV473;SAR86 clade ASV3515;E01-9C-26 marine group
ASV7713;Synechococcus sp.
ASV1302;NS5 marine group
ASV6017;Synechococcus sp.
ASV7530;unc. Rhodobacteraceae
ASV5567;SAR116 clade
ASV7591;SV1-8
ASV4832;Candidatus Actinomarina sp.
ASV4667;SAR11 subclade IIIa.2
ASV7214;unc. Acidimicrobiaceae
ASV5716;HIMB59 type
ASV1566;unc. Saprospiraceae
ASV3029;unc. Rickettsiales
ASV7518;LSUCC0101 type
ASV459;SAR406 clade
ASV7223;SAR116 clade
ASV1783;NS5 marine group
ASV1389;OM43 clade
ASV1334;NS5 marine group
ASV7245;unc. Methylophilaceae
ASV4651;Candidatus Pelagibacter sp.
ASV4540;unc. Alphaproteobacteria
ASV5387;NS5 marine group
ASV7027;MWH-UniPo type
ASV3952;NS4 marine group
ASV1106;SAR116 clade
ASV4672;SAR11 subclade IIIa.2
ASV6516;HIMB11 type
ASV5606;OM60/NOR5 clade
ASV6693;OM43 clade
ASV267;Candidatus Actinomarina
ASV1000;BAL58 clade
ASV1118;SAR116 clade
ASV5512;OM252 clade
ASV1505;OM60/NOR5 clade
ASV3349;NS5 marine group
ASV7657;aclV clade
ASV7609;acl clade
ASV7629;SAR11 LD12
ASV7613;acl clade
ASV7471;SAR11 subclade IIIa.1
ASV7735;acl clade
ASV7760;SAR11 clade
ASV7108;SAR11 subclade IIIa
ASV7241;OM43 clade
ASV5716;HIMB59 type
ASV6770;unc. Holophagaceae
ASV7420;acl clade
ASV6590;aclV clade
ASV7713;Synechococcus sp.
ASV5060;aclV clade
ASV7779;SAR11 subclade I
ASV7731;BAL58 clade
ASV2241;acl clade
ASV7025;MWH-UniPo type
ASV5387;NS5 marine gorup
ASV1817;acl clade ASV7146;MWH-
ASV7146;MWH-UniPo type
ASV5787;unc. Opitutae
ASV1142;SAR86 clade
ASV3353;unc. Gammaproteobacteria
ASV3971;unc. Sporichthyaceae
ASV2995;aclV clade
ASV7707;Candidatus Aquiluna sp.
ASV5003;unc. Betaproteobacteria
ASV6293;SAR11 clade
ASV2234;MWH-UniPo type
ASV7252;LD28 clade
ASV5396;unc. Gammaproteobacteria
ASV3167;acl clade
ASV6466;unc. Betaproteobacteria
ASV7027;MWH-UniPo type
ASV510;acl clade
ASV7150;Candidatus Actinomarina sp.
ASV3173;acl clade
ASV7245;unc. Methylophilaceae
ASV2671;Opitutus sp.
ASV7249;unc. Burkholderiaceae
ASV7591;SV1-8
ASV6014;Algoriphagus sp.
ASV3891;unc. Bacteria
ASV566;acl clade
ASV4829;Owenweeksia sp.
ASV2733;NS3a marine group
ASV4880;unc. Actinobacteria
ASV2238;acl clade
Phylum
Acidobacteria
Actinobacteria
Bacteroidetes
Cyanobacteria
Gemmatimonadetes
Proteobacteria
unclassified
verrucomicrobia
Salinity
30
20
10
0

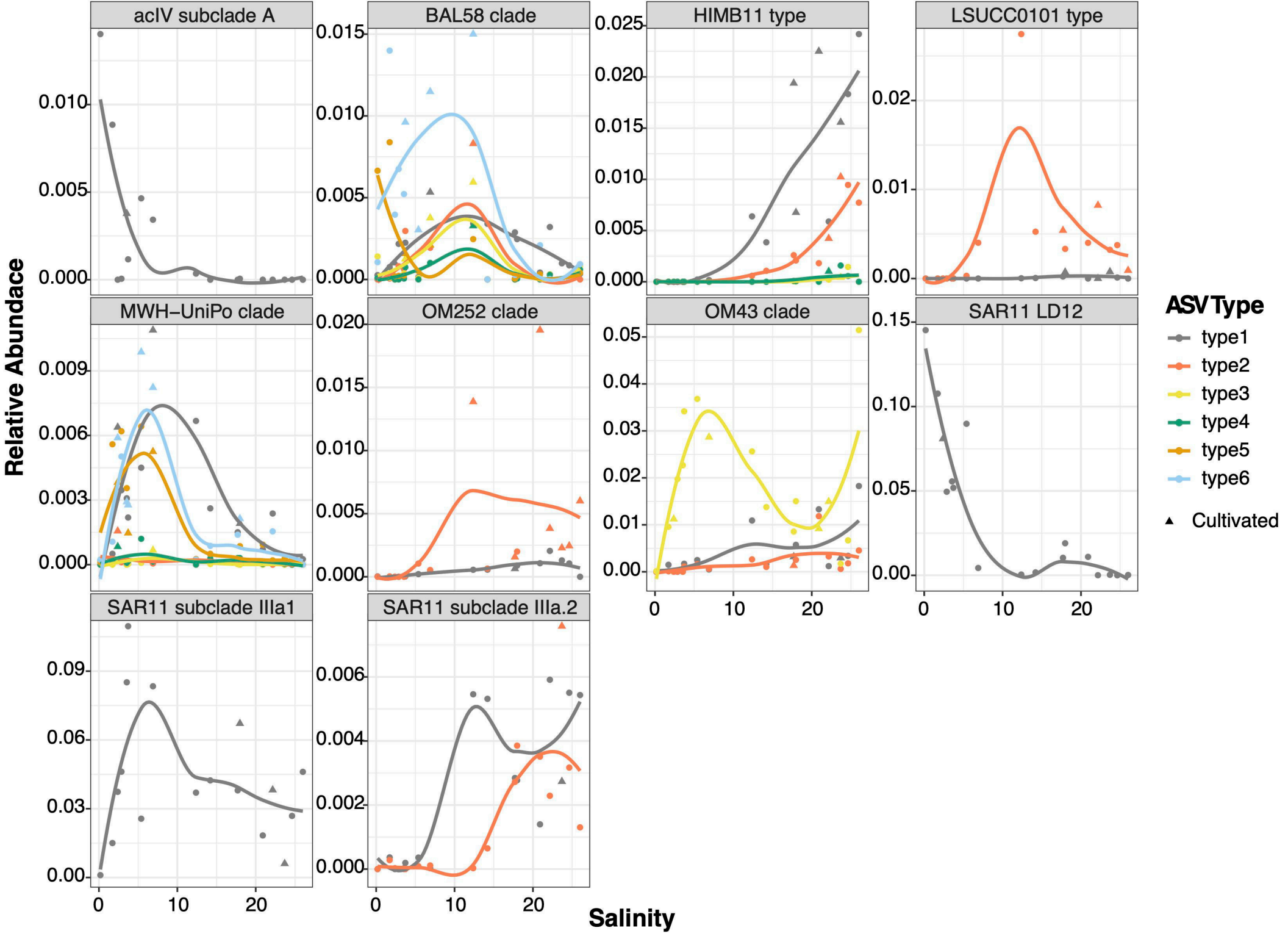
acIV subclade A
BAL58 clade
HIMB11 type
LSUCC0101 type
MWH−UniPo clade
OM252 clade
OM43 clade
SAR11 LD12
SAR11 subclade IIIa1
SAR11 subclade IIIa.2
Relative Abundace
Salinity
ASV Type
type1
type2
type3
type4
type5
type6
Cultivated

Step 1: Simulate *n* wells

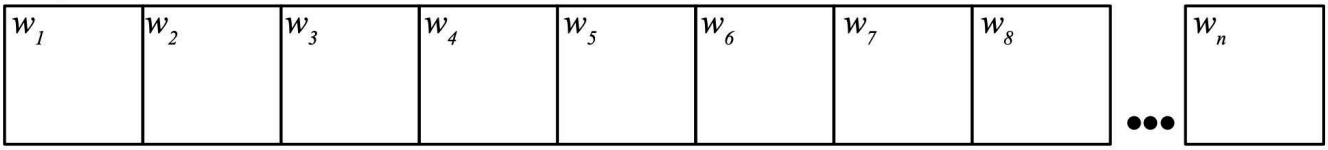

Step 2: Simulate inoculation of wells from Poisson distribution (λ=inoculum)

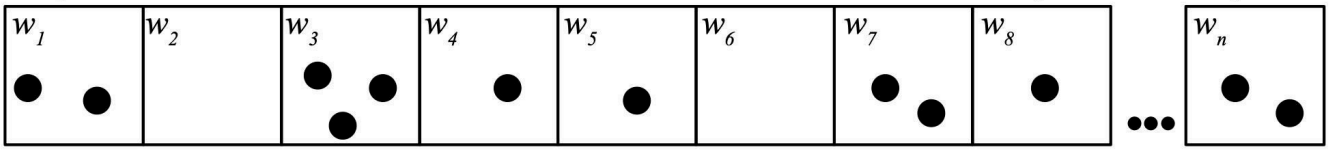

Step 3: Simulate likelihood of taxon from Binomial distribution (n = # cells in well, p = rel. abund)

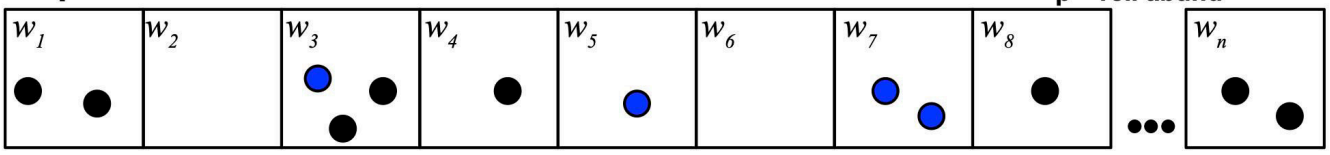

Step 4: Count positive wells, taxon positive wells, pure wells and taxon pure wells

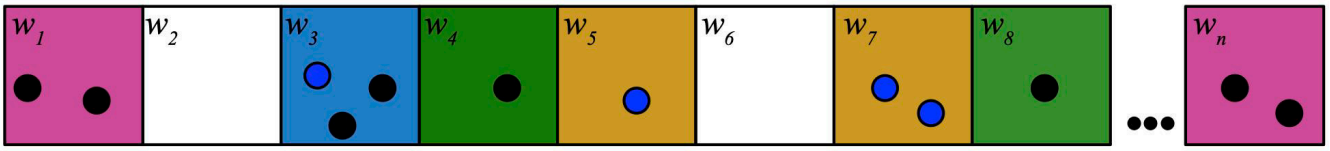

Step 5: For taxon pure wells, simulate likelihood of viability from Binomial distribution (n = # cells in well, p = viability)

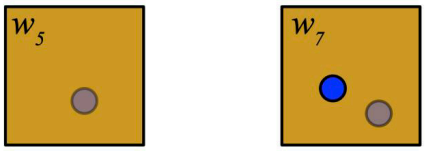

Step 6: Count wells where viable cells >=1

Step 7: Bootstrap steps 1-6 *k* times at different levels of viability, *0 ≤ v ≤ 1*

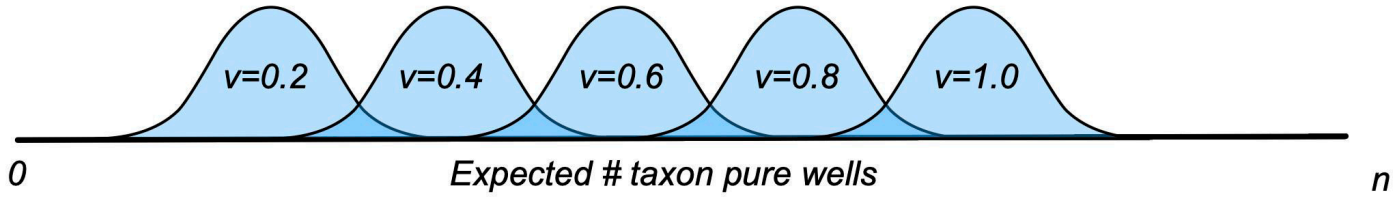

Step 8: Identify *min, max* values of *v* where # observed wells falls within bootstrapped 95% CI

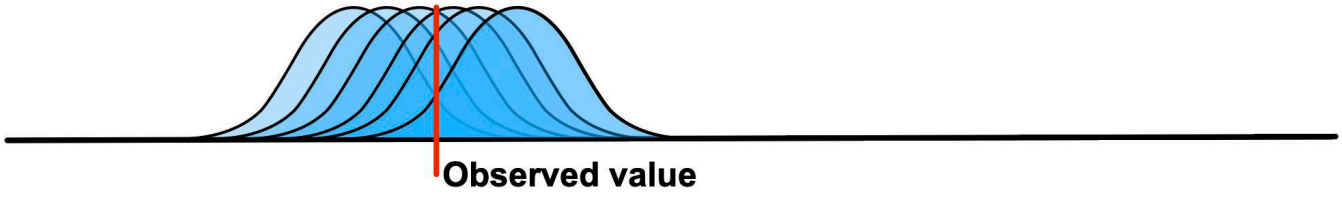

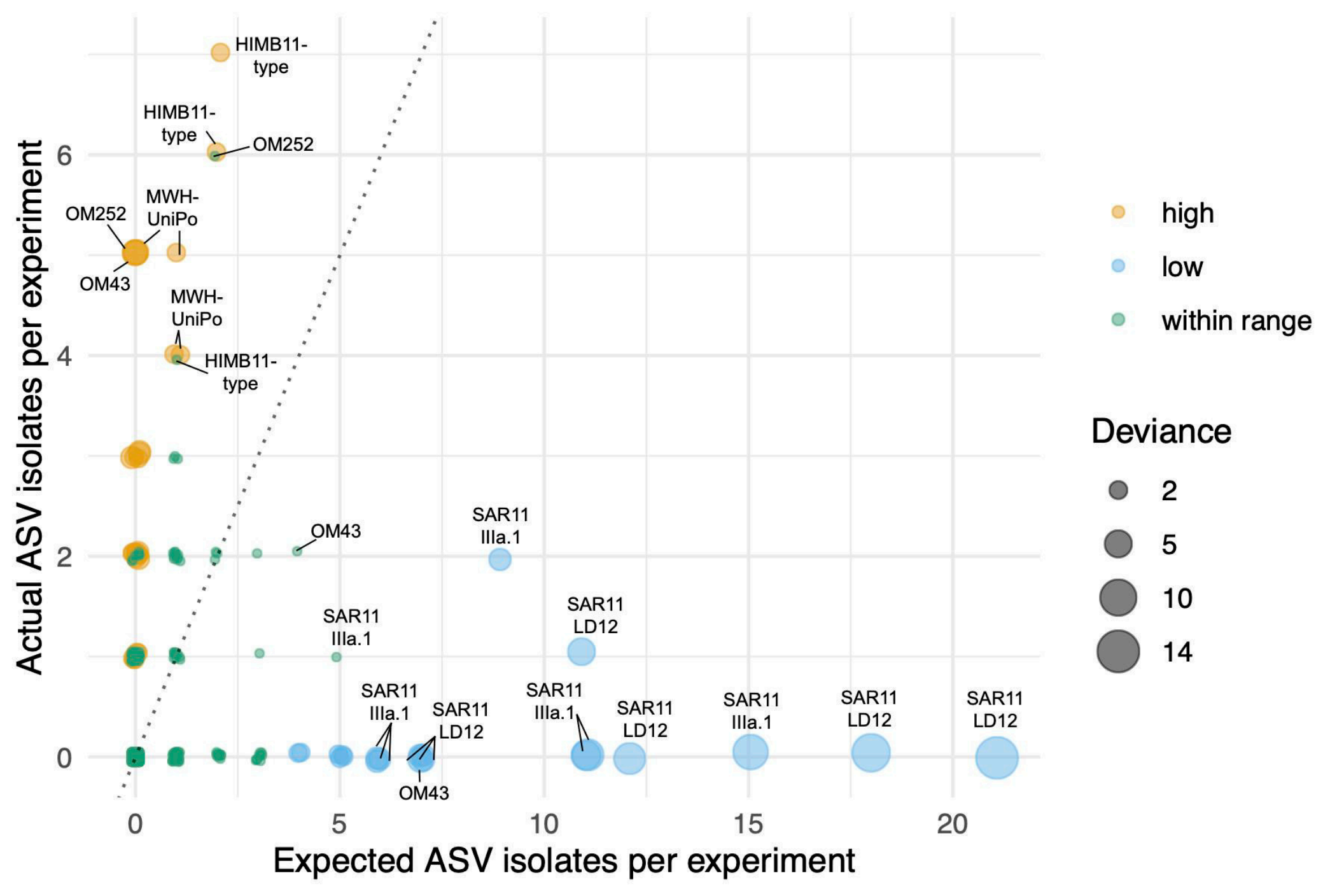
HIMB11-type
HIMB11-type
OM252
OM252
MWH-UniPo
OM43
MWH-UniPo
HIMB11-type
OM43
SAR11 IIIa.1
SAR11 IIIa.1
SAR11 LD12
SAR11 IIIa.1
SAR11 LD12
SAR11 LD12
SAR11 IIIa.1
SAR11 LD12
SAR11 LD12
SAR11 IIIa.1
SAR11 LD12
OM43
Actual ASV isolates per experiment
Expected ASV isolates per experiment
0
2
4
6
0
5
10
15
20
high
low
within range
Deviance
2
5
10
14